Molecular Microbiology (2016) 100(5), 841–859 ■
doi:10.1111/mmi.13354
First published online 23 March 2016

Mitogen activated protein kinases SakA^{HOG1} and MpkC collaborate for *Aspergillus fumigatus* virulence

Ariane Cristina Mendes de Oliveira Bruder Nascimento,[1] Thaila Fernanda dos Reis,[1] Patrícia Alves de Castro,[1] Juliana I. Hori,[1] Vinícius Leite Pedro Bom,[1] Leandro José de Assis,[1] Leandra Naira Zambelli Ramalho,[2] Marina Campos Rocha,[3] Iran Malavazi,[3] Neil Andrew Brown,[4] Vito Valiante,[5] Axel A. Brakhage,[6] Daisuke Hagiwara[7] and Gustavo H. Goldman[1]*

[1]*Faculdade de Ciências Farmacêuticas de Ribeirão Preto, Universidade de São Paulo, Ribeirão Preto, Brazil.*
[2]*Faculdade de Medicina de Ribeirão Preto, Universidade de São Paulo, Ribeirão Preto, Brazil.*
[3]*Departamento de Genética e Evolução, Centro de Ciências Biológicas e da Saúde, Universidade Federal de São Carlos, São Carlos, São Paulo, Brazil.*
[4]*Plant Science and Crop Biology, Rothamsted Research, Harpenden, Hertfordshire, UK.*
[5]*Leibniz Junior Research Group Biobricks of Microbial Natural Product Syntheses, Leibniz Institute for Natural Product Research and Infection Biology-Hans Knöll Institute, Jena, Germany.*
[6]*Department of Molecular and Applied Microbiology, Leibniz Institute for Natural Product Research and Infection Biology (HKI), Jena, Germany; Institute for Microbiology, Friedrich Schiller University, Jena, Germany.*
[7]*Medical Mycology Research Center, Chiba University, Chiba, Japan.*

Summary

Here, we investigated which stress responses were influenced by the MpkC and SakA mitogen-activated protein kinases of the high-osmolarity glycerol (HOG) pathway in the fungal pathogen *Aspergillus fumigatus*. The Δ*sakA* and the double Δ*mpkC* Δ*sakA* mutants were more sensitive to osmotic and oxidative stresses, and to cell wall damaging agents. Both MpkC::GFP and SakA::GFP translocated to the nucleus upon osmotic stress and cell wall damage, with SakA::GFP showing a quicker response. The phosphorylation state of MpkA was determined post exposure to high concentrations of congo red and Sorbitol. In the wild-type strain, MpkA phosphorylation levels progressively increased in both treatments. In contrast, the Δ*sakA* mutant had reduced MpkA phosphorylation, and surprisingly, the double Δ*mpkC* Δ*sakA* had no detectable MpkA phosphorylation. *A. fumigatus* Δ*sakA* and Δ*mpkC* were virulent in mouse survival experiments, but they had a 40% reduction in fungal burden. In contrast, the Δ*mpkC* Δ*sakA* double mutant showed highly attenuated virulence, with approximately 50% mice surviving and a 75% reduction in fungal burden. We propose that both cell wall integrity (CWI) and HOG pathways collaborate, and that MpkC could act by modulating SakA activity upon exposure to several types of stresses and during CW biosynthesis.

Accepted 11 February, 2016. *For correspondence. E-mail ggoldman@usp.br; Tel./Fax 55-16-33154280/81.

Introduction

All living organisms are subjected to stress during their normal life cycle. Fungal saprophytes and pathogens have evolved mechanisms to counteract this diverse array of stresses. On the cell surface, protein sensors perceive environmental signals, such as a change in pH, osmolarity, or the presence of xenobiotics, triggering intracellular signalling events that culminate with the activation of transcriptional regulators and the expression of specific gene targets. Fungal pathogens of humans are constantly exposed to stress and have to quickly adapt to different microenvironments within their host. Hence, the coordination of fungal stress responses is paramount for the successful establishment of infection (Brown and Goldman, 2016).

Aspergillus fumigatus is a major opportunistic pathogen and allergen of mammals (Greenberger, 2002, Dagenais and Keller, 2009), causing approximately 65% of all invasive fungal infections in humans, while being the

mostly encountered species accounting for pulmonary infections (Brown *et al.*, 2012a,b; Lackner and Lass-Florl, 2013). *A. fumigatus* causes several of clinical diseases including the life-threatening disease invasive pulmonary aspergillosis (IA), which has high mortality rates as high as 80% in neutropenic patients (Brakhage, 2005; Brown *et al.*, 2012a,b; Lackner and Lass-Florl, 2013). There is a general consensus that aspergillosis is a multifactorial disease with several phenotypes influencing the final outcome of the disease establishment (Tekaia and Latgé, 2005; Hartmann *et al.*, 2011; Sugui *et al.*, 2014). Factors involved in the establishment of the infection, include hypoxia resistance, iron assimilation, gliotoxin production (depending on the immune status of the host), presence of dihydroxynaphthalene melanin and thermophily (Hartmann *et al.*, 2011; Schrettl and Haas, 2011; Wezensky and Cramer, 2011; Carberry *et al.*, 2012; Grahl *et al.*, 2012; Scharf *et al.*, 2012; Heinekamp *et al.*, 2013; Moore, 2013; Chotirmall *et al.*, 2014; Ding *et al.*, 2014; Haas, 2014). However, it is essential to understand how these traits are coordinated in response to an environmental cue. Hence, a deep understanding of the signalling pathways that regulate these factors involved in virulence is needed.

The highly conserved mitogen-activated protein kinase (MAPK) signalling pathways are essential to the adaptation to environmental changes (Pearson *et al.*, 2001; Rispail *et al.*, 2009). The MAPK cascades are important for relaying, integrating and amplifying intracellular signals, and are crucial signalling components involved in many cellular processes (Pearson *et al.*, 2001; Rispail *et al.*, 2009). In filamentous fungi the conserved MAPK pheromone response, filamentous growth, osmotic stress response and cell wall integrity (CWI) pathways have been shown to influence numerous virulence traits including invasive growth, biofilm formation, mycotoxin production and antifungal tolerance (Bahn *et al.*, 2005; Monge *et al.*, 2006; Román *et al.*, 2007). *A. fumigatus* has four MAPKs: (i) MpkA, the central regulator of CWI pathway also plays a role in oxidative stress (Valiante *et al.*, 2015a; Du *et al.*, 2006), (ii) MpkB is the putative homologue of filamentous growth/pheromone response pathway, still uncharacterized and (iii) MpkC and SakA, homologues of the *Saccharomyces cerevisiae* Hog1, constitute the main regulator of the high osmolarity glycerol response (HOG) pathway (Maeda *et al.*, 1994). The MpkC protein sequence is very similar to that of SakA (at DNA level: 69.7% identity, e-value 3e-121; at protein level: 68.4% identity, 82.9% similarity, e-value: 2e-147). SakA and MpkC have also been shown to play a role in caspofungin adaptation and carbon source utilization, respectively (Reyes *et al.*, 2006; Altwasser *et al.*, 2015; Valiante *et al.*, 2015a). The *A. fumigatus* osmotic stress, HOG, pathway is composed of two signalling modules: (i) the two-component system (TCS)-like phosphorelay module composed of a hybrid sensor kinase (TcsC/NikA), a histidine-containing phosphotransfer (HPt) protein (YpdA) and a response regulator (RR, SskA) and (ii) the mitogen-activated protein (MAP) kinase module comprising of a MAP kinase kinase kinase (MAPKKK, SskB), MAP kinase kinase (MAPKK, PbsB) and MAP kinase (MAPK, SakA). The TCS senses and relays environmental signals that subsequently activate the Hog1 MAPK pathway which mediates the cellular response (Bahn, 2008; Ma and Li, 2013, Hagiwara *et al.*, 2013).

We have been investigating *A. fumigatus* MAPKs and their importance for the establishment of virulence/pathogenicity and mediation of drug resistance (Valiante *et al.*, 2008, 2009, 2015a,b; de Castro *et al.*, 2014; Altwasser *et al.*, 2015; Winkelströter *et al.*, 2015a,b; Bom *et al.*, 2015). Here, we expand this work by investigating the roles played by the two Hog1 homologues, SakA and MpkC, in different stress responses. In addition to the role played in the osmotic stress response, these paralogues were shown to perform a function in the CWI pathway and demonstrated to collaborate during virulence in a neutropenic murine model of invasive pulmonary aspergillosis.

Results

SakA *and* MpkC *play a role in osmotic, oxidative and temperature stress resistance*

The single and double *mpkC* and *sakA* mutants were previously constructed to investigate stress tolerance in conidia of *A. fumigatus* (Hagiwara *et al.*, 2014). Here, we expand this investigation by exploring which stress responses are mediated by these MAP kinases during mycelial growth and development. The corresponding wild-type strain and null mutants were grown in solid and liquid minimal media (MM) supplemented with increasing concentrations of sorbitol to induce osmotic stress (Fig. 1). In solid medium, the radial growth of the Δ*sakA* and Δ*mpkC* Δ*sakA* strains was significantly reduced in all three sorbitol concentrations when compared to the wild-type and complemented strains (Fig. 1A). However, in liquid medium the Δ*sakA* and Δ*mpkC* Δ*sakA* mutants have significant reduced growth in liquid medium only at MM + 0.6 M sorbitol when compared with the wild-type and complemented strains (Fig. 1B). Additionally, the Δ*sakA* and Δ*mpkC* Δ*sakA* mutant strains were more sensitive to oxidative stress induced by H_2O_2 or *t*-butyl hydroperoxide, but not paraquat, than the wild-type and complemented strains (Supporting Information Fig. S1 for all three oxidative stressing agents and Table S1 for *t*-butyl hydroperoxide and paraquat). The Δ*sakA* mutant also demonstrated a reduction

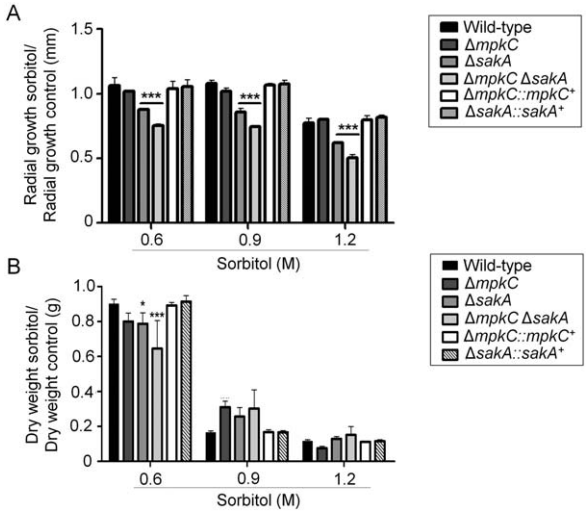

Fig. 1. The double mutant Δ*mpkC* Δ*sakA* is more sensitive to osmotic stress. Growth of wild-type and the MAP kinase null mutant strains on MM. The data are expressed as radial growth sorbitol/radial growth control (mm) (A). Dry weight of the wild type and the MAP kinase null mutant strains in MM with increasing concentrations of Sorbitol. The data are expressed as dry weight sorbitol/dry weight control (g) (B).The cultures were grown for 48 h at 37°C. The dry weight data are expressed as average ± standard deviation of three independent biological repetitions (* and *** denote $p < 0.05$ and 0.001, respectively, by *t*-tests when compared to the wild-type strain).

in growth (radial diameter) in solid MM at 50°C, while the double Δ*mpkC* Δ*sakA* had increased radial diameter at 44 and 50°C when compared to the wild-type strain (Supporting Information Fig. S2).

In *A. fumigatus* the TcsC/NikA histidine kinase, which is upstream of the HOG pathway, is involved in fungicide resistance and osmotic stress tolerance (McCormick *et al.*, 2012; Hagiwara *et al.*, 2013). Subsequently, the impact of phenylpyrrole and dicarboximide fungicides, fludioxonil and iprodione, respectively, of the various *A. fumigatus* strains was evaluated (Supporting Information Fig. S3 for radial growth and Table S1 for Minimal Inhibitory Concentrations, MICs). The Δ*sakA* and Δ*mpkC* Δ*sakA* mutant strains were more resistant to iprodione and fluodioxonil than the wild-type strain (Supporting Information Fig. S3 and Table S1).

To assess the involvement and sub-cellular location of MpkC and SakA in the osmotic stress response, we generated MpkC::GFP and SakA::GFP strains that use their endogenous promoters by replacing the wild-type alleles and behaved identically to the wild-type strain (Supporting Information Fig. S4 and data not shown). When the MpkC::GFP and SakA::GFP strains were grown in minimal medium for 16 h at 30°C, a very weak and diffuse fluorescent signal was observed in the cytosol (Figs. 2 and 3). In contrast, when transferred to MM plus 1.0 M sorbitol, MpkC::GFP accumulated in the nucleus 60 and 120 min post transfer, while SakA::GFP progressively accumulated in the nucleus as early as post 10 min exposure (Figs. 2 and 3). Hoechst counter staining confirmed the nuclear localization of the GFP signal. This suggests that SakA was important for a rapid response to osmotic stress, while MpkC was important for later events.

Collectively, this data suggests that both the *A. fumigatus* MAPKs of the HOG pathway, MpkC and SakA, collaborate in multiple stress responses, while SakA appears to play the major role.

SakA *and* MpkC *are involved in paradoxical growth, the CWI pathway and biofilm formation*

Alterations in the osmotic properties can affect the composition and structure of the cell wall (Altwasser *et al.*, 2015; Bom *et al.*, 2015; Valiante *et al.*, 2015a; Winkelströter *et al.*, 2015a). In accordance, the Δ*sakA* and Δ*mpkC* Δ*sakA* mutants were more sensitive to cell wall damaging agents, such as calcofluor white (CFW), congo red (CR) and to the cell membrane disruptor Sodium Dodecyl Sulfate (SDS) (Fig. 4 and Supporting Information Table S1 for MICs). The Δ*mpkC*, Δ*sakA* and Δ*mpkC* Δ*sakA* mutants were more sensitive to the β-1,3-glucan synthase and chitin synthase inhibitors, caspofungin and nikkomycin Z, respectively, when compared to the wild-type, and complemented strains (Fig. 5A and B, and Supporting Information Table S2 for Minimal Effective Concentrations, MECs). The wild-type and the Δ*mpkC* were able to grow in higher caspofungin concentrations of 4–8 μg ml^{-1}, a phenomenon described as a paradoxical effect or trailing (i.e., the escape of *A. fumigatus* from caspofungin inhibition at concentrations above the MIC; Chen *et al.*, 2011; Fig. 5A). Interestingly, in the Δ*sakA* and Δ*mpkC* Δ*sakA* mutants this effect was partially decreased (Fig. 5A). As an indirect approach to investigate the composition of the mutant cell walls, mycelia were subjected to enzymatic hydrolysis with Lallzyme MMX and the resulting protoplasts counted as a measure of cell wall digestibility. Digestion of the Δ*sakA* and Δ*mpkC* Δ*sakA* mutants yielded approximately 50% less protoplasts than the wild-type, Δ*mpkC* and complemented strains (Fig. 5C) indicating that the Δ*sakA* and Δ*mpkC* Δ*sakA* mutant cell wall was much more susceptible to the enzymatic degradation. This suggests that the cell wall of the Δ*sakA* and Δ*mpkC* Δ*sakA* mutants possessed a modified carbohydrate composition. As already previously shown, Δ*mpkA* defective in the CWI MAPK pathway produced a far higher number of protoplasts than the corresponding wild-type strain (Rocha *et al.*, 2015; Fig. 5C).

The reduced sensitivity of the Δ*sakA* and Δ*mpkC* Δ*sakA* mutants to enzymatic digestion suggested that

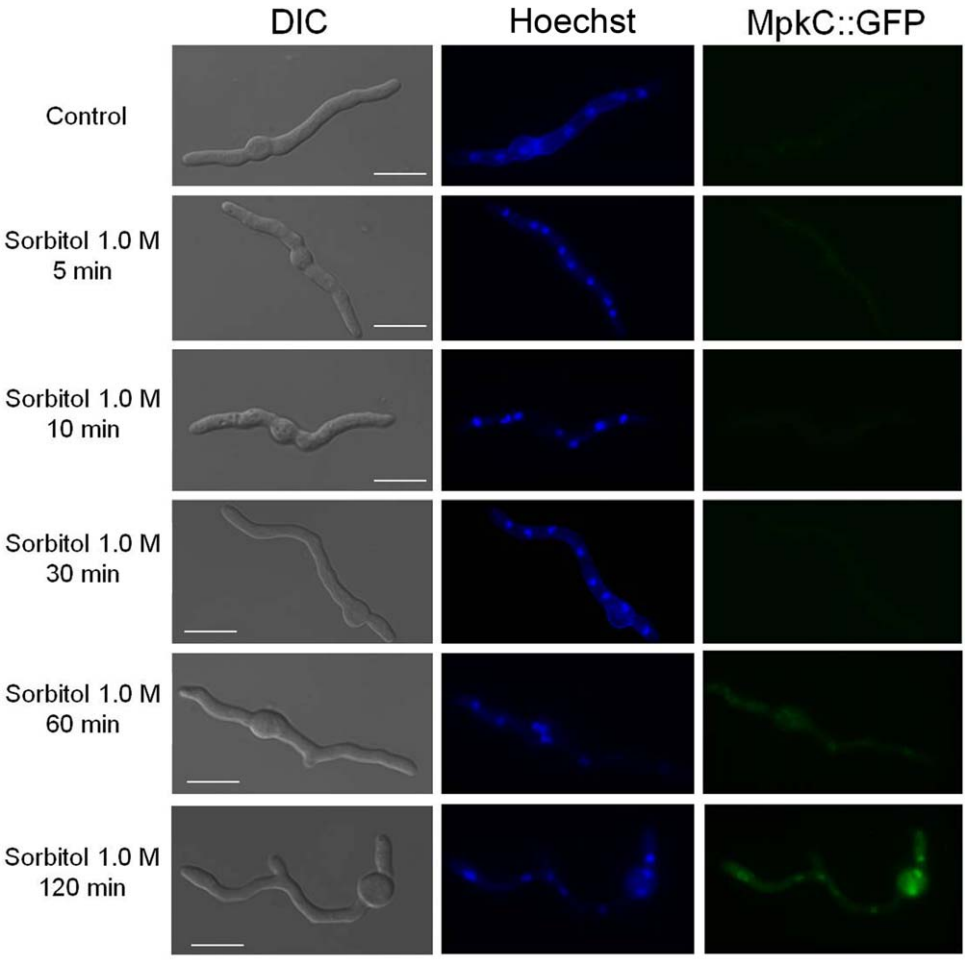

Fig. 2. MpkC::GFP accumulates in the nuclei upon osmotic stress. The MpkC::GFP strain was grown for 16 h at 30°C in MM and afterwards incubated for 5, 10, 30, 60 and 120 min in the presence of 1.0 M sorbitol. Bars, 5 μm.

these strains possessed alterations in cell wall composition. Subsequently, CFW and soluble dectin-1 staining were used to identify differences in the content, or exposure, of chitin and β-glucans on the surface of the fungal cell wall. The intensity of CFW staining per fungal area was 30% higher in Δ*mpkC* mutant than wild-type and complemented strains, while Δ*sakA* and Δ*mpkC* Δ*sakA* were 20% lower than wild-type and complemented strains (Fig. 6A, left panel). The Δ*mpkC*, Δ*sakA* and Δ*mpkC* Δ*sakA* mutant strains were shown to have more abundant β-glucans than the wild-type and complemented strains. The intensity of dectin-1 staining per fungal area was 50, 40 and 30% higher in the mutants compared with wild-type strain (Fig. 6A, right panel). Collectively, these results suggest that the surface of the Δ*mpkC* and Δ*sakA* strains had altered β-1,3 glucans and chitin compared with wild-type strain. The altered composition of the cell wall could also alter the adhesion of conidia and mycelia to abiotic and biotic surfaces or other fungal cells. In turn, the ability of the respective mutants to form biofilms on solid surfaces was assessed. Adhesion was evaluated by crystal violet (CV) staining and was shown to be decreased by approximately 80% (in 0.1% glucose) and 70% (in 1.0% glucose) in Δ*sakA* and Δ*mpkC* Δ*sakA* mutants respectively (Fig. 6B).

To determine if the MpkC and SakA were involved in the Mpk1 pathway in *A. fumigatus*, the amount and state of phosphorylation of Mpk1p homologue, MpkA, were determined in the presence and absence of CR (15, 30 and 60 min) and sorbitol (10 min) stresses. The phosphorylation level of the MpkA protein was determined using the antiphospho-p44/42 MAPK antibody directed against phosphorylated MpkA (MpkA-P). This antibody recognizes a single band in the wild-type and no band in the Δ*mpkA* mutant (Figs. 7 and 8). In the wild-type strain, MpkA phosphorylation levels were progressively increased in both treatments (Fig. 7). The Δ*mpkC* mutant demonstrated levels of MpkA phosphorylation similar to the wild-type strain (Fig. 7A and B). In contrast, the Δ*sakA* mutant had reduced MpkA phosphorylation (Fig. 7A and C), and surprisingly, the double Δ*mpkC* Δ*sakA* had no detectable MpkA phosphorylation (Fig. 7A and D). We have also performed a different set of experiments keeping the time of stressing conditions constant and changing the

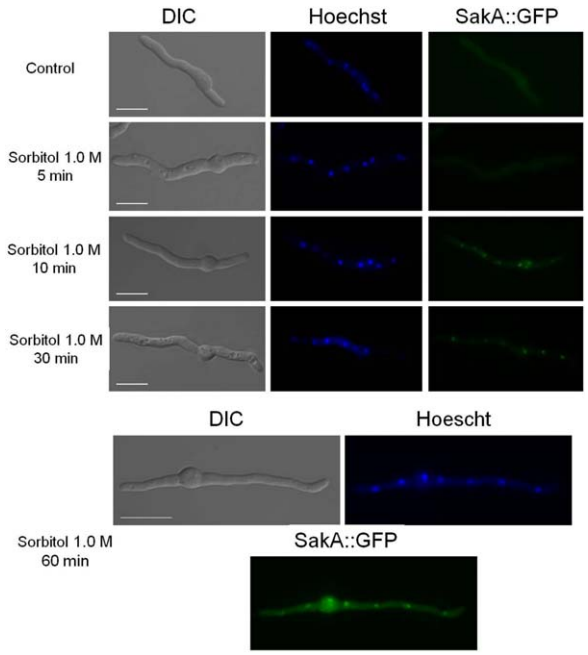

Fig. 3. SakA::GFP accumulates in nuclei upon osmotic stress. The SakA::GFP strain was grown for 16 h at 30°C in MM and incubated for 5, 10, 30 and 60 min in the presence of 1.0 M sorbitol at 30°C. Bars, 5 μm.

concentration of either CR or sorbitol (Fig. 8A–D). In lower CR and Sorbitol concentrations, MpkA phosphorylation can still be observed but in very high concentrations the results are comparable to those observed in Fig. 7 (Fig. 8A–D). In all these experiments, in addition to measure the phosphorylation levels of the MpkA protein we also determined the total levels of non-MpkA-P by using the anti-p44/42 MAPK antibody. In all treatments, non-MpkA-P showed constant levels (Figs. 7 and 8).

The sub-cellular location of MpkC and SakA was assessed during exposure to cell wall stress. When the MpkC::GFP and SakA::GFP strains were grown in minimal medium (MM) for 16 h at 30°C, they showed a very weak and diffuse fluorescence signal in the cytosol (Figs. 9 and 10). In contrast, when transferred to MM + caspofungin 0.125 μg ml^{-1} for between 5 and 60 min, MpkC::GFP and SakA::GFP progressively accumulated in the nucleus, which was confirmed by Hoechst costaining (Fig. 9A–C). Collectively, this demonstrates that MpkC and SakA collaborate in the CWI pathway.

SakA *and* MpkC *collaborate during* A. fumigatus *virulence*

The importance of MpkC and SakA for *A. fumigatus* pathogenicity was evaluated in a neutropenic murine model of invasive pulmonary aspergillosis (Fig. 11A). There are no statistical differences among the wild-type, Δ*mpkC* and Δ*sakA* (by using two different statistical tests, Log−rank Mantel−Cox and Gehan−Breslow−Wilcoxon). Wild-type infection resulted in 100% mortality 6 days post-infection, while Δ*mpkC* infection resulted in a significantly mortality rate of 70% after 15 days post-infection (Fig. 11A). Virulence was restored in an independent strain that resulted from a single ectopic reintegration of the wild-type *mpkC* gene. There was no statistical difference between the wild-type and the complemented Δ*mpkC::mpkC*$^{+}$ strain (Fig. 11A). The Δ*sakA* infection resulted in a significantly mortality rate of 100% after 15 days post-infection (Fig. 11B). Virulence was restored in an independent strain that resulted from a single ectopic reintegration of the wild-type *sakA* gene. Also in this case there was no statistical difference between the wild-type and the complemented Δ*sakA::sakA*$^{+}$ strain (Fig. 11B).

The Δ*mpkC* Δ*sakA* infection resulted in the greatest reduction in mortality rate, with only 45% of mice dying after 15 days post-infection (Fig. 11C, $p < 0.0049$ and $p < 0.0079$ for the comparison between the wild-type and the double null mutant, Log−rank Mantel−Cox and Gehan−Breslow−Wilcoxon tests respectively).

Histopathological examination revealed that at 72 h post-infection the lungs of mice infected with the wild-type strain contained multiple foci of invasive hyphal growth, which penetrated the pulmonary epithelium in major airways, while pockets of branched invading hypha originated from the alveoli (Fig. 12A, left panel and insets). In contrast, Δ*mpkC* Δ*sakA* infections revealed inflammatory infiltrates in bronchioles, with some containing poorly germinated or non-germinated conidia (Fig. 12A, right panel). Fungal burden was measured by qPCR, showing that the Δ*mpkC*, Δ*sakA*, Δ*mpkC* Δ*sakA*, strains have reduced fungal growth within the lungs compared to the wild-type and the complemented Δ*mpkC::mpkC*$^{+}$ and Δ*sakA::sakA*$^{+}$ strains (Fig. 12B). Taken together, these results clearly demonstrate that both MpkC and SakA play an important role in *A. fumigatus* virulence, while the dual absence of both kinases has an additive effect.

The impaired Δ*mpkC* and Δ*sakA* CWI together with the dramatic attenuation in virulence could contribute to an altered immune response. Subsequently, the cytokine Tumour Necrosis Factor alpha (TNF-α) levels released from bone marrow derived macrophages (BMDMs) after co-incubation with *A. fumigatus* hyphae were investigated. TNF-α is an important inflammatory mediator secreted by macrophages when exposed to *A. fumigatus* (Taramelli *et al.*, 1996; Hayashi *et al.*, 2005). BMDMs co-cultured with either Δ*sakA* or Δ*mpkC* Δ*sakA* showed higher TNF-α production than the wild-type or the complemented strains (approximately 1.5-fold, Fig. 12C). These results suggest that the effect caused by the absence of SakA or the dual absence of SakA and

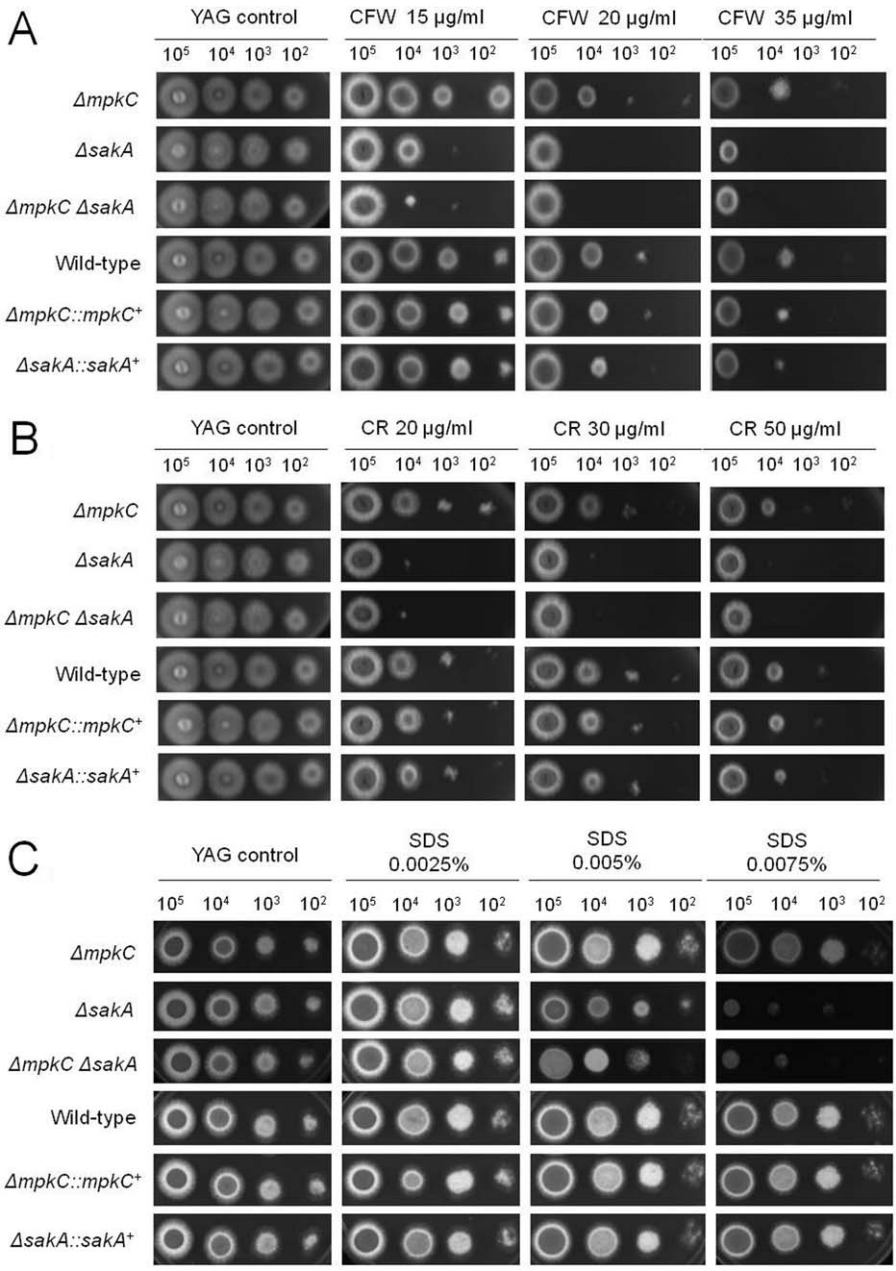

Fig. 4. The Δ*sakA* and Δ*mpkC* Δ*sakA* mutant strains are more sensitive to cell wall damaging agents. The wild type, the mutant, and the complemented strains were grown on YAG medium with increasing concentrations of calcofluor white, CFW (A), congo red, CR (B), and Sodium Dodecyl Sulfate, SDS (C) for 48 h at 37°C.

MpkC on the CWI is important for macrophage recognition and inducing inflammatory responses.

Discussion

The Hog1 MAPK pathway in *S. cerevisiae* is responsible for the adaptation to hyperosmotic stress, the production of the osmolyte glycerol, alterations in gene expression and short-term cell cycle arrest (for reviews, see Rispail *et al.*, 2009; Saito and Posas, 2012; Brewster and Gustin, 2014). In general, the inactivation of Hog1, or its orthologues in other fungi, increases the sensitivity of the respective fungus to hyperosmotic stress (for reviews, see Rispail *et al.*, 2009; Saito and Posas, 2012; Brewster and Gustin, 2014). Besides its role in the regulation of hyperosmotic stress, the *S. cerevisiae* Hog1 pathway has also been shown as associated to other stresses (Rodrígues-Peña *et al.*, 2010), such as oxidative stress (Bilsland *et al.*, 2004), acid stress (Lawrence *et al.*, 2004, Mollapour and Piper, 2006), methylglyoxal (Aguilera *et al.*, 2005), temperature downshift (Panadero *et al.*, 2006), arsenite (Thorsen *et al.*, 2006), cesium chloride (Del Vescovo *et al.*, 2008), heat shock (Winkler *et al.*,

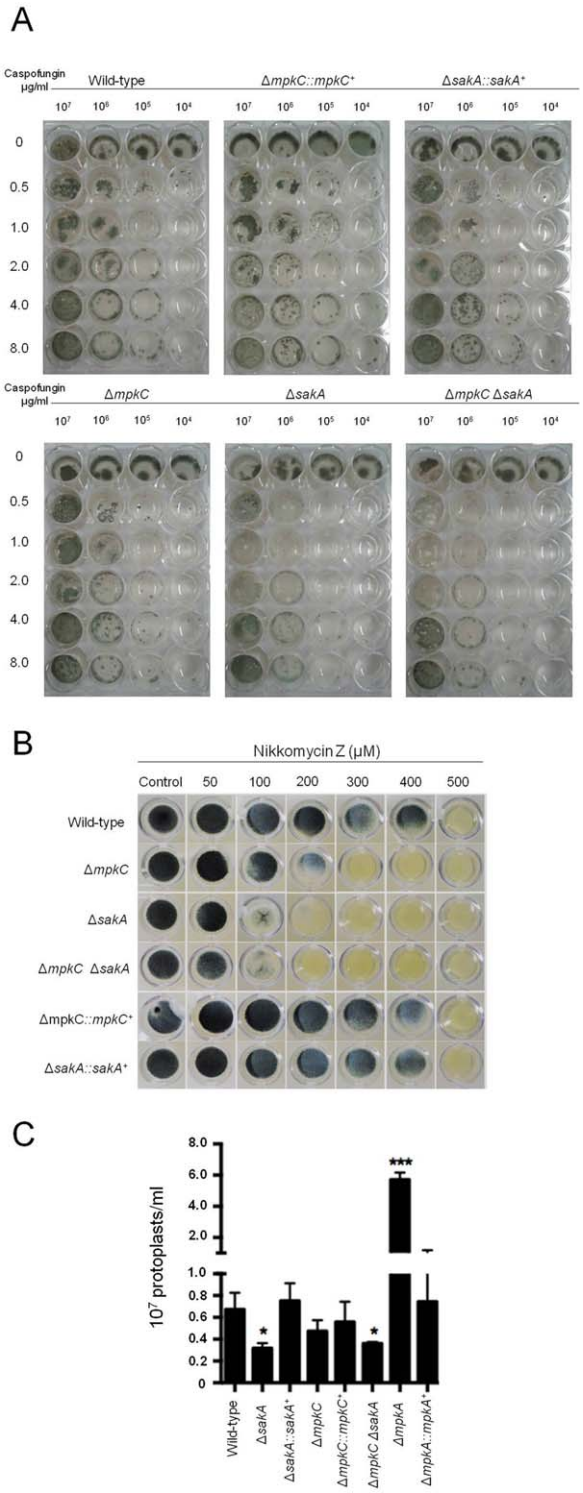

Fig. 5. The Δ*sakA* and Δ*mpkC* Δ*sakA* mutant strains display increased sensitivity to caspofungin and nikkomycin Z, and decreased protoplast production.
A. Growth of wild-type, the MAP kinase null mutant, and complemented strains on YG medium with increasing concentrations of caspofungin. The cultures were grown for 60 h at 37°C.
B. Growth of wild-type, the MAP kinase null mutant, and complemented strains in YG medium with increasing concentrations of Nikkomycin Z. The cultures were grown for 72 h at 37°C.
C. Protoplasts releasing from wild-type, the MAP kinase null mutant, and complemented strains mycelia. The digestion mixture included the Lallzyme MMX and 100 mg of mycelium in 50 ml of osmotic stabilizer solution. Protoplasts were quantified using a Neubauer chamber (* and *** denote $p < 0.05$ and 0.001, respectively, by *t*-tests when compared to the wild-type strain).

2002) and zymolyase (Bermejo *et al.*, 2008). In other fungi, the multifunctional role of the orthologous HOG pathway is also observed, such as *Candida albicans* where Hog1 is involved in numerous stress responses including osmotic, oxidative, iron, cell wall, ergosterol, in addition to white-opaque switching and mating (Kaba *et al.*, 2013; Thomas *et al.*, 2013; Liang *et al.*, 2014; Komalapriya *et al.*, 2015; Ene *et al.*, 2015).

Here, we investigated the multifunctional roles of the two *A. fumigatus* Hog1 orthologues, MpkC and SakA. These two MAPKs are possible paralogues and very limited information is available concerning their roles in *A. fumigatus* pathogenicity. Both MAPKs were shown to be important not only for osmotic stress, but also for oxidative stress, cell wall damage and heat shock. The simultaneous disruption of both MAPKs had an additive effect, as the Δ*mpkC* Δ*sakA* double mutant showed increased sensitivity to the aforementioned stresses in comparison to the single Δ*mpkC* and Δ*sakA* mutants. In the majority of cases, the stress phenotypes of Δ*mpkC* were moderate, while the phenotypes of Δ*sakA* were more drastic. In *S. cerevisiae*, Hog1 mutants were highly resistant to phenylpyrrole and dicarboximide fungicides (Segmuller *et al.*, 2007; Lin and Chung, 2010; Van Thuat *et al.*, 2012). However, here the *A. fumigatus* Δ*sakA* and Δ*mpkC* Δ*sakA* mutants were only slightly more resistant to fluodioxonil, but not to iprodione. Therefore, both the *A. fumigatus* HOG orthologues, SakA and MpkC function in multiple stress responses, while SakA appears to play the major role.

The Δ*sakA* mutant was more sensitive to cell wall damaging agents, such as CFW, CR, SDS, Lallzyme and caspofungin, while sensitivity of the Δ*mpkC* mutant was comparable to that of the wild-type strain. However, the double Δ*mpkC* Δ*sakA* mutant was more sensitive to these agents than the Δ*sakA* mutant, strongly indicating these two MAPKs both participate in the CWI pathway. Consistently, SakA and MpkC were translocated into the nucleus when germlings were challenged either with osmotic stress or caspofungin. During exposure to both osmotic stress and cell wall damage, SakA::GFP was earlier present in the nucleus than MpkC::GFP. However, the migration of MpkC::GFP to the nucleus appeared to be quicker post cell damage caused by

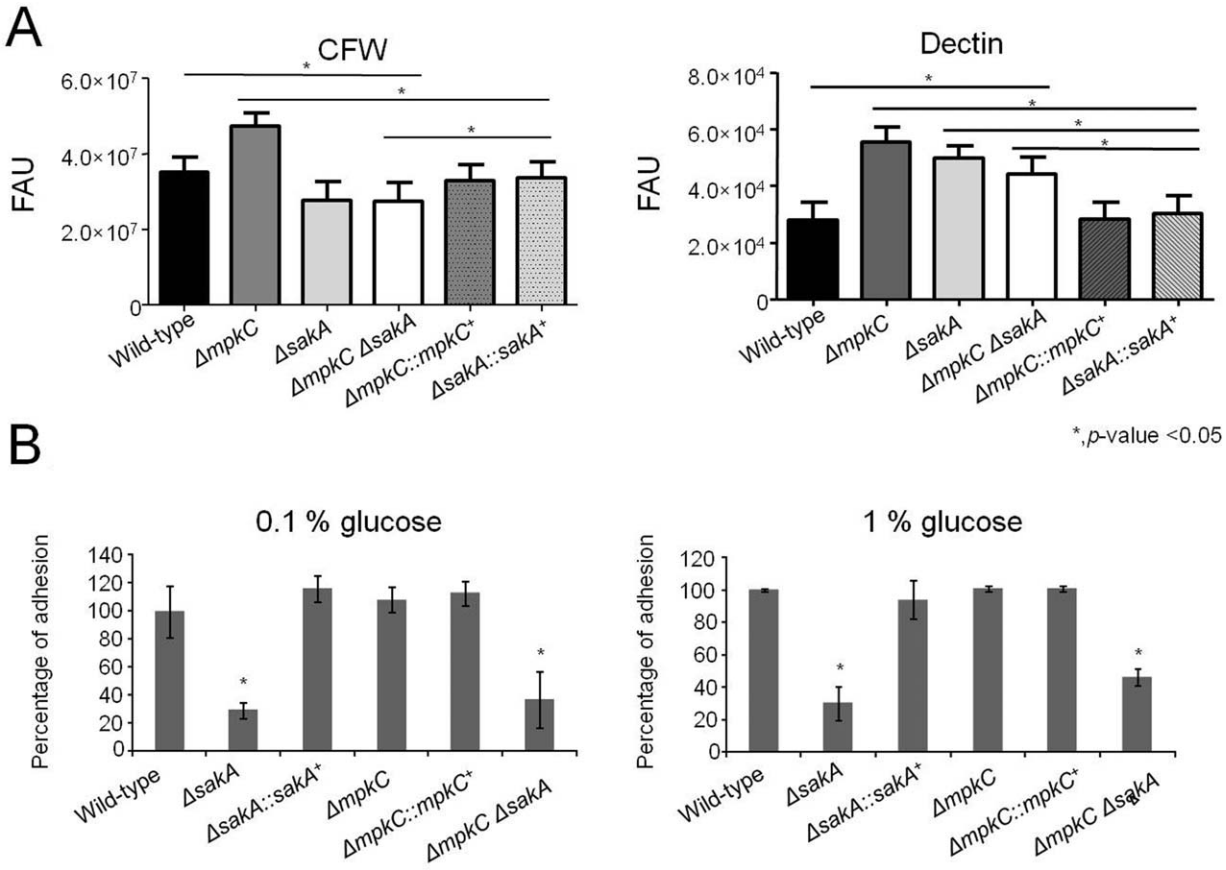

Fig. 6. Detection of the β-1,3 – glucan and chitin content on the cell surface. Conidia were cultured in liquid media to the hyphal stage, UV-killed, and stained with calcofluor white (CFW) or soluble dectin-1 to detect the content of exposed chitin or β-glucan (A) respectively. The intensity of staining was calculated by averaging the amount of staining to the total area of each fungal cell using ImageJ software. These experiments were performed in triplicate, and the results are displayed as mean values with standard errors (* denotes $p < 0.05$ by *t*-tests, when compared to the wild-type strain). (B) Adhesion measured by Crystal Violet (CV) assay is reduced in the Δ*sakA* and Δ*mpkC* Δ*sakA* mutant strains in both 0.1% (w/v) and 1% (w/v) glucose (*, denotes $p < 0.05$ by *t*-tests when compared to the wild-type strain). FAU, Fluorescence Arbitrary Units.

caspofungin. Previously, by a systems biology approach Altwasser *et al*. (2015) demonstrated that increased concentrations of caspofungin promoted activation and cross talk between the *A. fumigatus* MpkA and SakA pathways. Caspofungin affected intracellular transport, causing an additional osmotic stress that was independent of glucan inhibition, but high concentrations of caspofungin reduced this osmotic stress. The authors showed that both MAPK pathways were very important for adaptation to caspofungin and also contribute to the paradoxical effect (Chen *et al*., 2011). Recently, Valiante *et al*. (2015b) showed that a newly discovered compound, humidimycin, affected the *A. fumigatus* HOG pathway. Simultaneous administration of humidimycin and caspofungin resulted in a synergistic increase in caspofungin efficacy, suggesting the existence of a potential salvage pathway acting during the caspofungin stress response. Taken together, the data presented here strongly indicates that MpkC and SakA are interacting during cell wall stress and thereby influencing the CWI pathway.

The contribution of MpkC and SakA to the CWI pathway was investigated by determining MpkA phosphorylation during osmotic stress and cell wall damage. Interestingly, MpkA phosphorylation progressively increased during increasing osmotic stress. In contrast, this MpkA response was reduced in the Δ*sakA* mutant, but absent in the Δ*mpkC* Δ*sakA* mutant in low or high osmotic stressing conditions. These results show that MpkA phosphorylation during osmotic stress was dependent on MpkC and SakA. Upon cell wall damage, MpkA phosphorylation progressively increased concomitantly with the CR concentration. In the Δ*mpkC* Δ*sakA* mutant MpkA phosphorylation increased at low CR concentrations, but was completely absent at high CR concentrations. This shows that MpkA phosphorylation was partially dependent on MpkC and SakA, relative to the degree of cell wall damage. Altwasser *et al*. (2015)

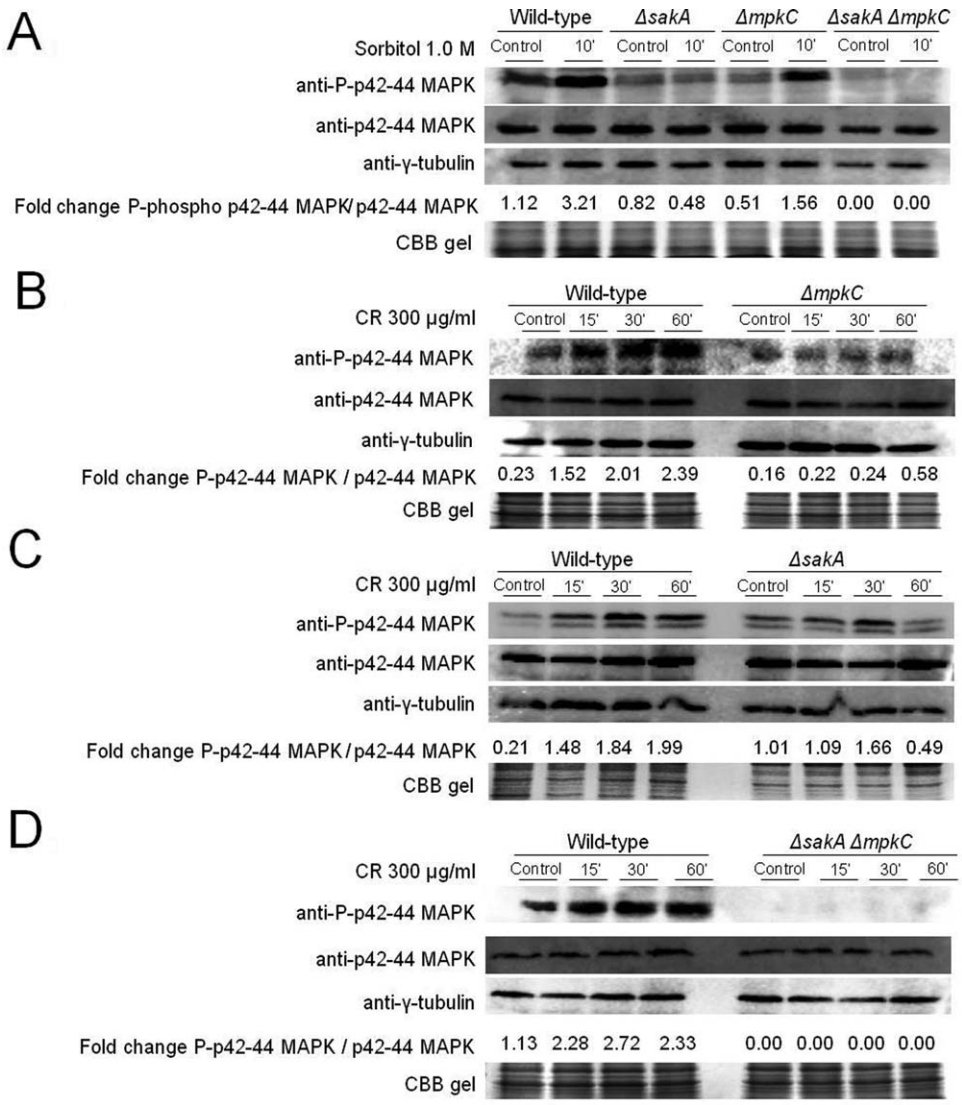

Fig. 7. *A. fumigatus* Δ*mpkC* Δ*sakA* mutant strain has no detectable MpkA phosphorylation upon osmotic and cell wall damage stresses. Immunoblot analysis for MpkA phosphorylation in response to sorbitol (A, C) and congo red, CR (B, D) stresses. The wild-type and the null mutant strains were grown in YAG for 18 h at 37°C. Then, sorbitol 1.0 M or CR (300 µg ml^{-1}) were not added (control) or added for 10 min (sorbitol) or 15, 30 and 60 min (CR). Anti-p44/42 MAPK or Anti-44/42 MAPK antibodies directed against phosphorylated MpkA and total MpkA were used to detect the phosphorylation of MpkA and total MpkA respectively. Anti-ϫ-tubulin antibody was used as a control for loading. A Coomassie Brilliant Blue (CBB)-stained gel is shown as an additional loading control. Signal intensities were quantified using the Image J software by dividing the intensity of MpkA-P/MpkA.

observed a significantly higher level of SakA phosphorylation after exposure to caspofungin in the Δ*mpkA* mutant. In accordance with what was observed in the present study on *A. fumigatus*, Altwasser *et al*. (2015) showed that MpkA phosphorylation dropped during caspofungin treatment in the Δ*sakA* mutant. Collectively, all presented data strongly indicates that the HOG pathway plays an important role during cell wall damage and its functionality is essential for the maintenance of the CWI pathway. Similarly to our observations, Altwasser *et al*. (2015) proposed that both pathways were activated during cell wall damage and that they were activated during the caspofungin paradoxical effect.

In animal and plant pathogenic fungi, such as *C. albicans, Cryptoccocus neoformans*, *Penicillium marneffei*, *Fusarium graminearum*, *Cochliobolus heterostrophus*, *Alternaria alternata*, *Cryphonectria parasítica, Botrytis cinerea*, Hog1 homologues were shown to be important for virulence (Alonso-Monge *et al*., 1999; Park *et al*., 2004; Bahn *et al*., 2005; Segmuller *et al*., 2007; Igbaria *et al*., 2008; Lin and Chung, 2010; Van Thuat *et al*., 2012; Nimmanee *et al*., 2015). In addition, Hog1 homologues are also important for full virulence in insect biocontrol fungi (such as *Beauveria bassiana* and *Metarhizium anisopliae*) and hyperparasites as *Trichoderma harzianum* (Delgado-Jarana *et al*., 2006; Zhang *et al*., 2009; Chen *et al*., 2014). Distinct from the aforementioned fungi, in *A. fumigatus* two Hog1 homologues exist. Here, we show that both the *A. fumigatus* Δ*sakA* and Δ*mpkC* were virulent in mouse survival experiments, but displayed a 40% reduction in fungal burden. In contrast, the double Δ*mpkC* Δ*sakA* mutant showed highly attenuated virulence. This attenuation is most likely not due to any growth defect of the double mutant

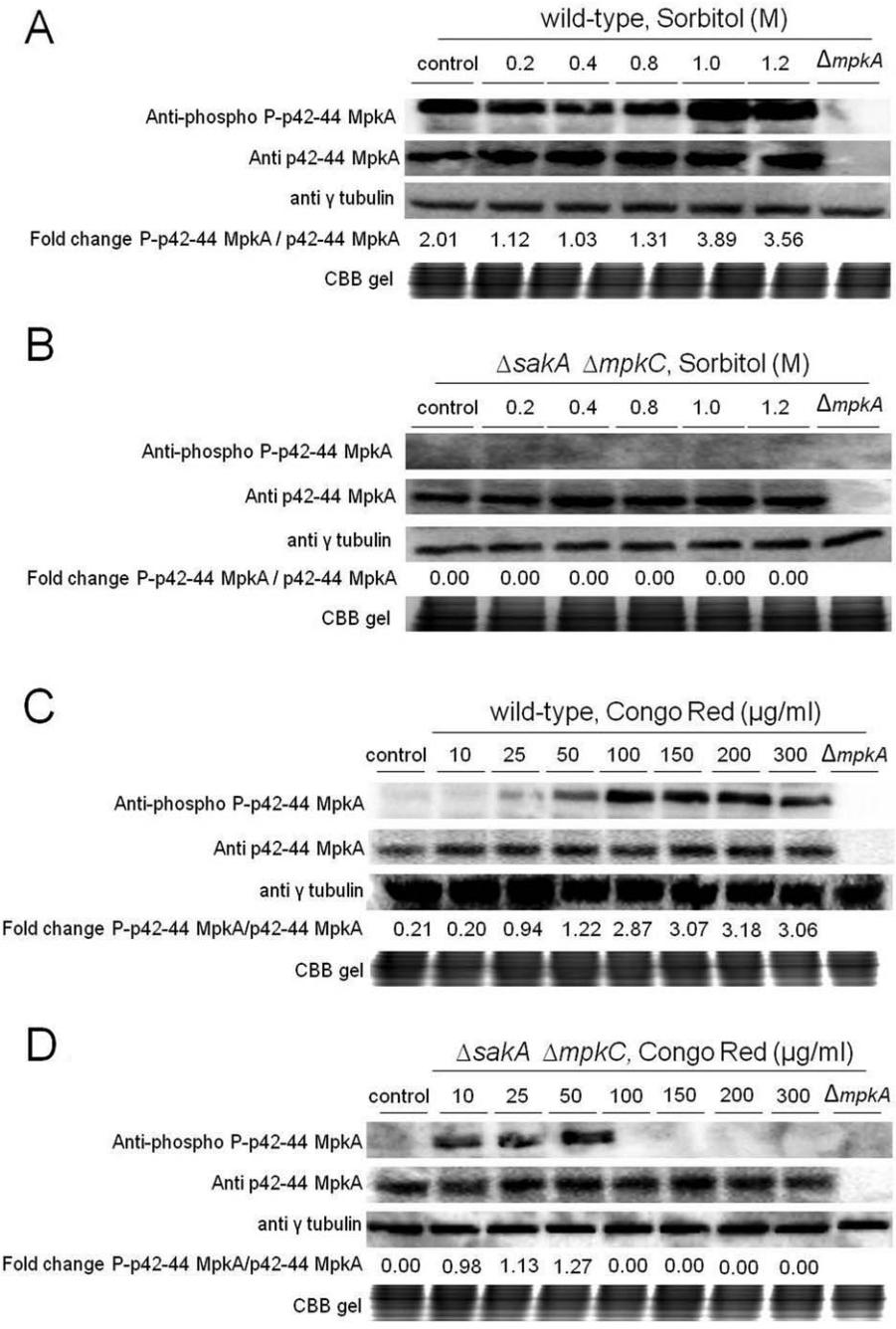

Fig. 8. *A. fumigatus* Δ*mpkC* Δ*sakA* mutant strain has no detectable MpkA phosphorylation upon osmotic and cell wall damage stresses. Immunoblot analysis for MpkA phosphorylation in response to sorbitol (A, C) and congo red, CR (B, D) stresses. The wild type and the null mutant strains were grown in YAG for 18 h at 37°C. Then, sorbitol 0.2, 0.4, 0.8, 1.0 or 1.2 M or congo red (10, 25, 50, 100, 150, 200 or 300 μg ml^{-1}) were not added (control) or added for 10 min (sorbitol) or 60 min (congo red). Anti-p44/42 MAPK or Anti-44/42 MAPK antibodies directed against phosphorylated MpkA and total MpkA were used to detect the phosphorylation of MpkA and total MpkA respectively. Anti-ϫ-tubulin antibody was used as a control for loading. A Coomassie Brilliant Blue (CBB)-stained gel is shown as an additional loading control. Signal intensities were quantified using the Image J software by dividing the intensity of MpkA-P/MpkA.

because on agar plates the double mutant grew at least as good as the Δ*sakA* and Δ*mpkC* mutants (Supporting Information Fig. S3). TNF-α, is one of the key inflammatory mediators secreted by macrophages in response to fungal hyphae, and TNF-α levels were increased in during infection by the Δ*sakA* and the double Δ*mpkC* Δ*sakA* strains. This pro-inflammatory cytokine plays an important role in the induction of the innate immune response to *A. fumigatus* (Taramelli *et al*., 1996; Hayashi *et al*., 2005). β-glucan is a potent stimulator of the TNF-α response in fungi (Hohl *et al*., 2005; Steele *et al*., 2005; Huang *et al*., 2009; Faro-Trindade *et al*., 2012). Therefore, the increased β-1,3 glucan in the cell wall of these mutants potentially contributed to the increased recognition of the pathogen by a mammalian dectin receptor, favoring its increased phagocytosis by alveolar macrophages, and consequently the increased production of TNF-α. Intriguingly, Δ*mpkC* also contained increased β-1,3 glucan in the cell wall but triggered a similar level of TNF-α production as the wild-type strain.

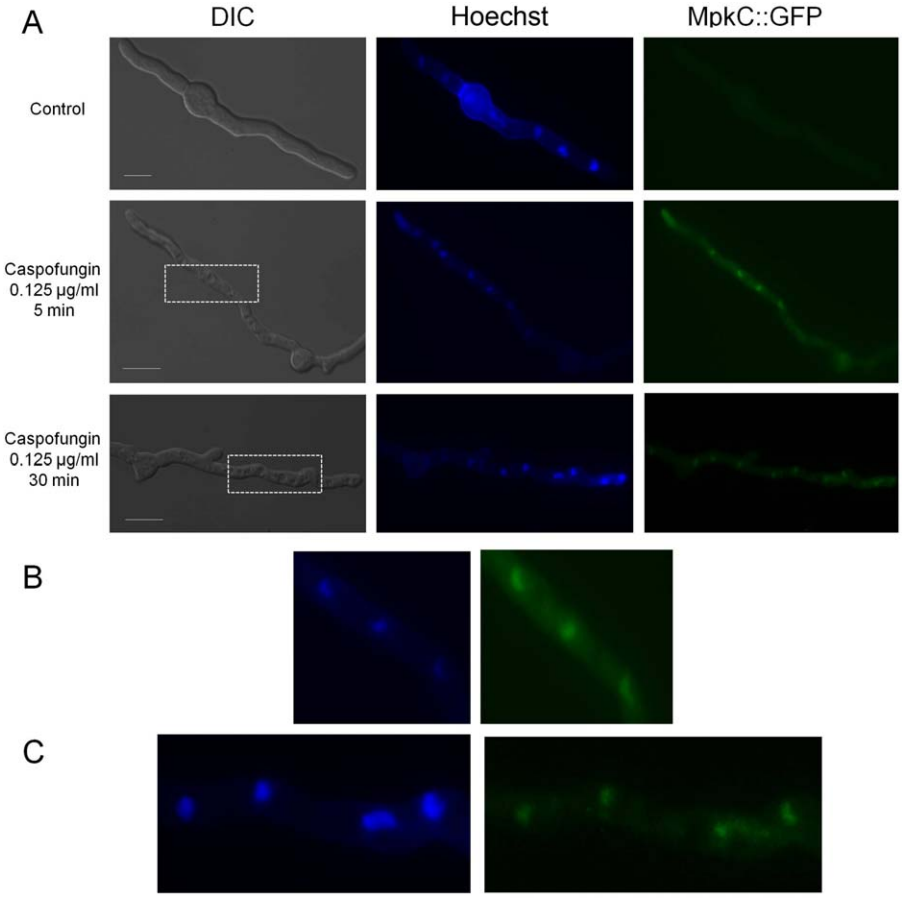

Fig. 9. MpkC::GFP accumulates in nuclei upon cell wall damage stress. The MpkC::GFP strain was grown for 16 h at 30°C in MM medium and incubated for 5 and 30 min in the presence of 0.125 µg ml^{-1} of caspofungin at 30°C (A). (B, C) show a close-up highlighted in a dashed white box in the treatment with caspofungin for 5 and 30 min in (A). Bars, 5 µm.

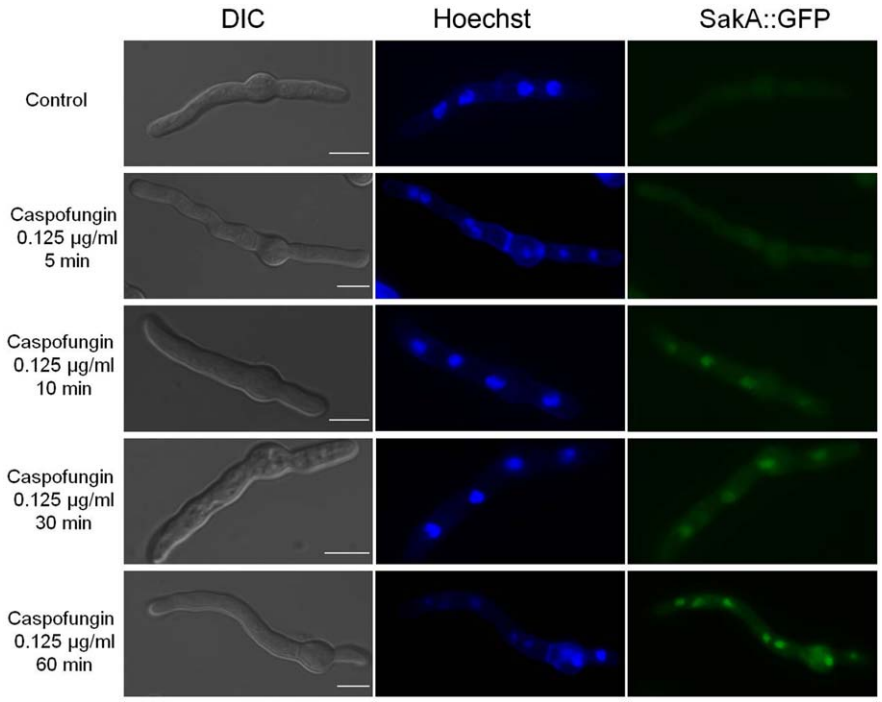

Fig. 10. SakA::GFP accumulates in nuclei upon cell wall damage stress. The SakA::GFP strain was grown for 16 h at 30°C in MM medium and incubated for 5, 10, 30 and 60 min in the presence of 0.125 µg ml^{-1} of caspofungin at 30°C. Bars, 5 µm.

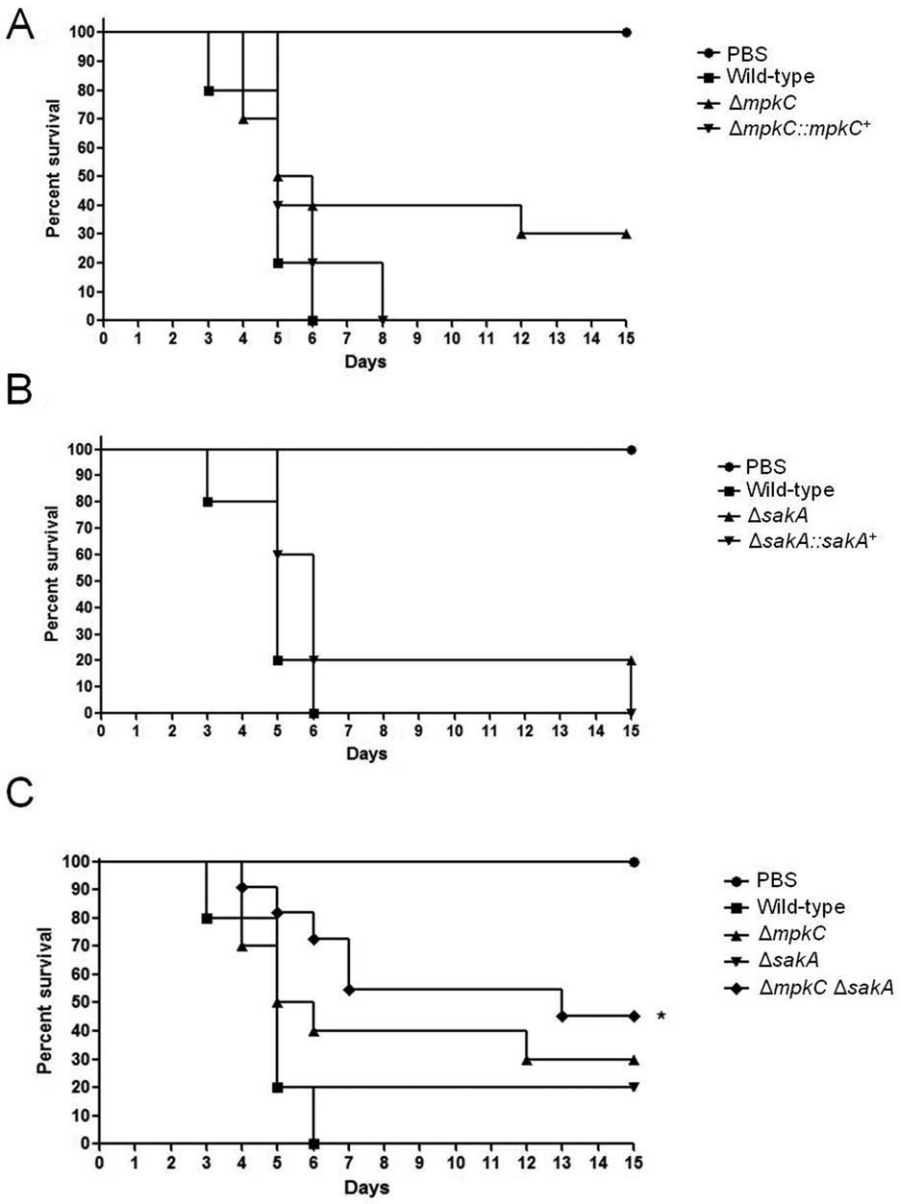

Fig. 11. *A. fumigatus* MpkC and SakA collaboration contributes to virulence in neutropenic mice.
A. Comparative analysis of wild type and mutant strains in a neutropenic murine model of pulmonary aspergillosis. Mice in groups of 10 per strain were infected intranasally with a 20 μl suspension of conidia at a dose of 10^5. (A) The Δ*mpkC* mutant compared to the wild type and Δ*mpkC::mpkC*$^+$ strains.
B. The Δ*sakA* mutant compared to the wild type and Δ*sakA::sakA*$^+$ strains.
C. The Δ*mpkC* Δ*sakA* mutant compared to the wild type, Δ*mpkC*, and Δ*sakA* strains. PBS, phosphate Buffer Saline; *, $p < 0.0049$ and $p < 0.0079$ for the comparison between the wild-type and the double null mutant, Log−rank, Mantel−Cox, and Gehan−Breslow−Wilcoxon tests respectively.

Because Δ*mpkC* has a higher chitin content than the wild-type strain, while Δ*sakA* and Δ*mpkC* Δ*sakA* mutants had lower chitin content than the wild-type strain, it is conceivable that the increased chitin content of the Δ*mpkC* mutant promoted alterations in the cell wall that masked β-1,3 glucan recognition by the dectin receptor.

In summary, we have identified an interaction between MpkC and SakA to counteract osmotic, oxidative, high temperature stresses, and also to regulate cell wall biosynthesis. Furthermore, this interaction is essential for virulence and macrophage recognition. It remains to be investigated how MpkC and SakA are affecting MpkA phosphorylation and the organization of the cell wall. Since most of the phenotypes observed for Δ*mpkC* were milder than for Δ*sakA* mutant, we propose that both the CWI and HOG pathways collaborate, and that MpkC could act by modulating SakA activity upon exposure to several different types of stress and during cell wall biosynthesis.

Experimental procedures

Ethics statement

The principles that guide our studies are based on the Declaration of Animal Rights ratified by the UNESCO in January 27, 1978 in its 8th and 14th articles. All protocols used

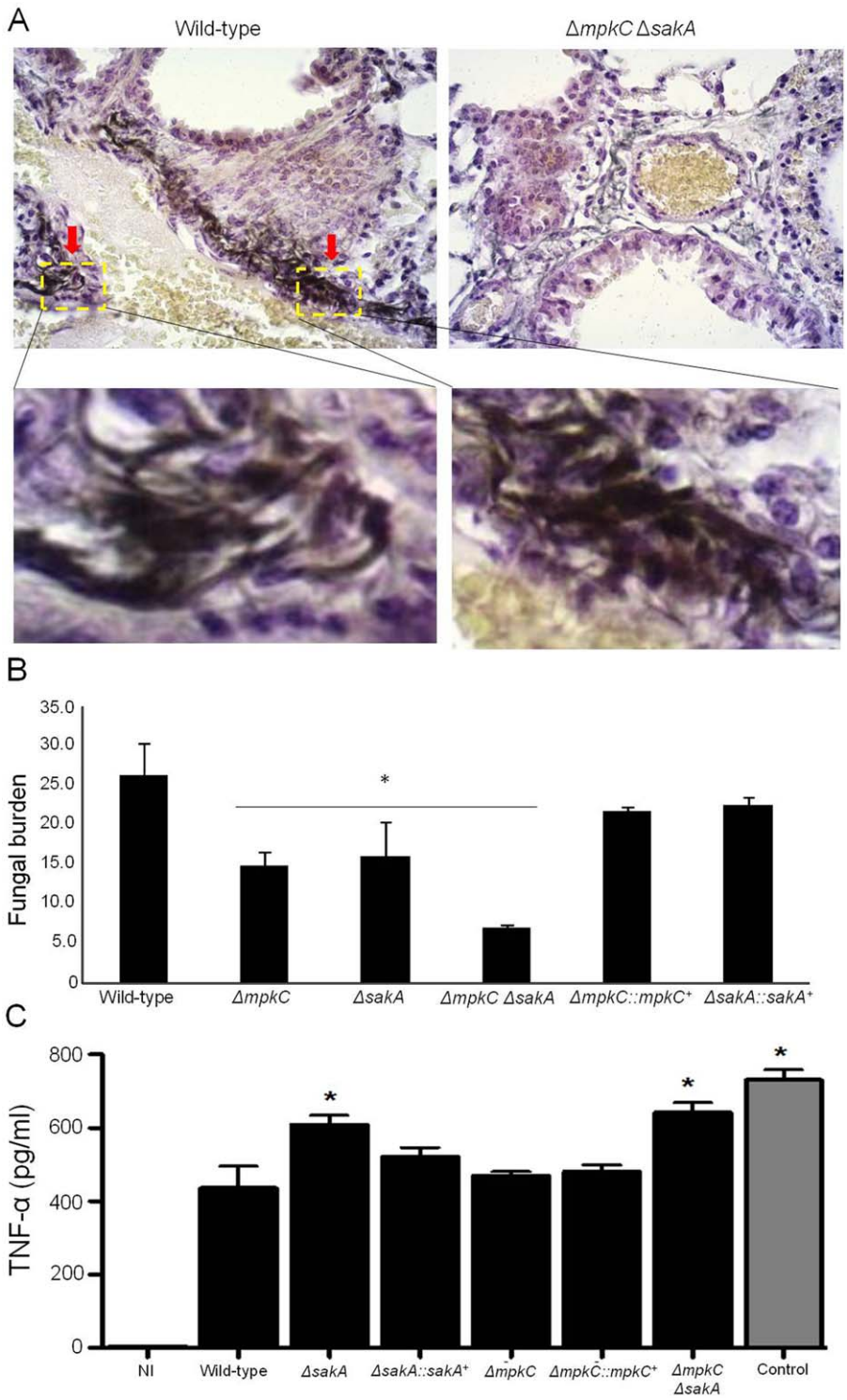

Fig. 12. *A. fumigatus* SakA and MpkC are important for macrophage recognition and inducing inflammatory responses.
A. Histological analysis of infection murine lung was performed 72 h after infection. The wild-type (left panel) is compared to the double mutant strain (right panel). For each sample, sequential 5-μm-thick sections were collected on glass slides and stained with Gomori methenamine silver (GMS) or hematoxylin and eosin (HE) stain. Red arrows show areas were germlings of the wild-type can be observed and are amplified in the insets.
B. Fungal burden was determined 72 h post-infection by real-time qPCR based on 18S rRNA gene of *A. fumigatus* and an intronic region of the mouse GAPDH gene. Fungal and mouse DNA quantities were obtained from the Ct values from an appropriate standard curve. Fungal burden was determined through the ratio between pg of fungal DNA and ng of mouse DNA. The results are the means (± standard deviation) of five lungs for each treatment. Statistical analysis was performed by using *t*-test (*, $p < 0.01$).
C. TNF−α secretion from bone marrow-derived macrophages (BMDMs). The Δ*sakA* and Δ*mpkC* Δ*sakA* strains trigger significantly increased release of TNF−α from BMDMs compared to wild type, Δ*mpkC*, and the reconstituted strain. BMDMs from C57BL/6 mice were infected with *A. fumigatus* hyphae for 18 h and the supernatant of cells was collected to measure the TNF-α levels by ELISA. Data show average ± SD and * denotes $p \leq 0.005$ compared to the wild type and the complemented strains. NI, Non−infected; Control, LPS (Lipolysaccharide, 1μg ml^{-1} for 18 h as a positive control).

in this study were approved by the local ethics committee for animal experiments from the Campus of Ribeirão Preto, Universidade de São Paulo (Permit Number: 08.1.1277.53.6; Studies on the interaction of *Aspergillus fumigatus* with animals). All animals were housed in groups of five within individually ventilated cages and were cared for in strict accordance with the principles outlined by the Brazilian College of Animal Experimentation (Princípios Éticos na Experimentação Animal – Colégio Brasileiro de Experimentação Animal, COBEA) and Guiding Principles for Research Involving Animals and Human Beings, American Physiological Society. All efforts were made to minimize

Table 1. Strains used in this work.

Strain	Genotype	Source
Afs35	Wild-type strain	FGSC A1159
CEA17	Wild-type strain	Our laboratory
Ku80	Δ*ku80::pyrG*AF	FGSCA1151
Ku80pyrG	Δ*ku80::pyrG*AF *pyrG*$^{-}$	Our laboratory
Δ*mpkC*	Δ*mpkC::prtA*	Hagiwara *et al.* (2014)
Δ*sakA*	Δ*sakA::hph*	Hagiwara *et al.* (2014)
Δ*mpkC* Δ*sakA*	Δ*mpkC::prtA* Δ*sakA::hph*	This work
Δ*mpkC::mpkC*$^{+}$	Δ*mpkC::mpkC*$^{+}$*::prtA*	This work
Δ*sakA::sakA*$^{+}$	Δ*sakA::sakA*$^{+}$*::prtA*	This work
SakA::GFP	*sakA::GFP::hph*	This work
MpkC::GFP	*mpkC::GFP::hph*	This work

suffering. Animals were clinically monitored at least twice daily and humanely sacrificed if moribund (defined by lethargy, dyspnoea, hypothermia and weight loss). All stressed animals were sacrificed by cervical dislocation.

Strains and media

The *A. fumigatus* strains used in this study are described in Table 1. To construct the complemented strains, Δ*mpkC::mpkC*$^{+}$ and Δ*sakA::sakA*$^{+}$, the plasmids, pSH75-mpkC+ and pPTRI-sakA+ were generated respectively. They include 2.0 and 1.4 kb of promoters, ORFs (*mpkC* and *sakA*), and 1.5 and 0.7 kb of terminator regions, respectively, which were generated as described previously using a GeneArt system (Invitrogen) and primers shown in Table S1 (Hagiwara *et al.*, 2013). The MpkC::GFP and SakA::GFP strains were generated using the primers and the strategies described in Supporting Information Table S3 and Fig. S4. Media were of two basic types. A complete medium with three variants: (2% (w/v) glucose, 0.5% (w/v) yeast extract, 2% (w/v) agar, trace elements), YUU (YAG supplemented with 1.2 g l^{-1} each of uracil and uridine) and liquid YG or YUU medium of the same composition (but without agar). A modified minimal medium (MM: 1% (w/v) glucose, original high nitrate salts, trace elements, 2% (w/v) agar, pH 6.5) was also applied. Trace elements, vitamins and nitrate salts were described by Kafer (1977).

Phenotypic assays

The phenotypes of the deletion mutants were evaluated either by radial growth or assessing the initial growth of a droplet of conidia from a serial dilution, at different temperatures, in the presence or absence of oxidative and osmotic stressing agents. Drop out experiments were performed using 5 μl of a 10-fold dilution series starting at a concentration of 2×10^7 for the wild-type and mutant strains spotted on different growth media and grown for 48 h at 37°C. The *A. fumigatus* CV assay was performed according to (Mowat *et al.*, 2007; Shopova *et al.*, 2013) respectively. All the experiments were performed at least three times.

Susceptibility was also determined by using antifungal MIC or MEC methods (CLSI, M38A2; http://clsi.org/) with an inoculum of 1×10^4 conidia. Microtiter plates were inoculated with a spore suspension, incubated at 37°C for 24–48 h, and read visually and with a spectrophotometer. MICs of the drugs were determined visually as a no-growth endpoint at 48 h of incubation. MECs was the lowest caspofungin or nikkomycin concentrations that led to the growth of small, rounded, compact microcolonies compared to hyphal growth in the growth control (nikkomycin or caspofungin-free RPMI-1640) after 48 h incubation. We have used MOPS [3-(*N*-morpholino)propanesulfonic acid] buffered RPMI (pH 7.0) 1640-2% glucose (Life Technologies). The different drugs were twofold diluted with the following range: (i) caspofungin (0.03 to 16 μg ml^{-1}); (ii) nikkomycin (500 nM to 0.97 uM); CR (0.4 to 1.6 μg ml^{-1}); (iii) CFW (0.4 to 1.6 μg ml^{-1}); (iv) SDS (0.00375 to 2%); (v) *t*-butyl hydroperoxide (0.03–16 mM); (vi) paraquat (0.15 to 80 mM); (vii) fludioxonil (0.005–2.5 μg ml^{-1}) and (viii) iprodione (0.02 to 10 μg ml^{-1}). Four repetitions were performed for each treatment.

Staining and microscopy

MpkC::GFP and SakA::GFP conidia were cultivated on coverslips in 4 ml of MM medium for 16 h at 30°C. After incubation, subsets of coverslips with adherent germlings were left untreated, treated with sorbitol 1.0 M or caspofungin 0.125 μg ml^{-1} for different periods of time. Subsequently, the coverslips were rinsed with phosphate-buffered saline (PBS; 140 mM NaCl, 2 mM KCl, 10 mM $NaHPO_4$, 1.8 mM KH_2PO_4, pH 7.4) and incubated for 3 min in a solution with Hoechst stain (Life Technologies) (12 μg ml^{-1}). After incubation with the dye, the coverslips were washed with PBS and mounted for examination. Slides were visualized on an Observer Z1 fluorescence microscope using a 100× objective oil immersion lens (for GFP, filter set 38 – high efficiency [HE], excitation wavelength of 450–490 nm, and emission wavelength of 525/50 nm; for Hoechst stain, filter set 49, excitation wavelength of 365 nm, and emission wavelength of 420–470 nm). Differential interference contrast images and fluorescent images were captured with an AxioCam camera (Carl Zeiss) and processed using AxioVision software (version 4.8).

Staining for dectin-1 and chitin

This procedure was performed as described by (Graham *et al.*, 2006; Winkelströter *et al.*, 2015a,b). Briefly, *A. fumigatus* conidia were grown for 6 h at 37°C, UV-irradiated, blocked using blocking solution (goat serum 2% (w/v), BSA 1% (w/v), 0.1% (v/v) Triton X-100, 0.05% (v/v) Tween 20, 0.05% (v/v) sodium azide and 0.01 M PBS) for 1 h at room temperature, and stained with conditioned medium containing 1 μg ml^{-1} of s-dectin-hFc followed by DyLight 594-conjugated, goat anti-human IgG1 (Graham *et al.*, 2006). For chitin staining, UV-irradiated germlings were treated with CFW 2 μg ml^{-1} for 5 min. After washing, stained cells were visualized under identical imaging conditions for parallel comparison using a Zeiss Observer Z1 fluorescence microscope.

Protoplast counting

To assess the ability of the different strains to generate protoplasts under standard conditions containing cell wall-degrading enzymes, 2×10^6 conidia from each strain were inoculated in 50 ml liquid YG and incubated for 16 hours at 37°C (180 rpm). Cells were washed twice with sterile MilliQ water and 100 mg of mycelium wet weight were incubated in 50 ml of a osmotic stabilized protoplasting solution [(0.4 M ammonium sulfate; 50 mM citric acid pH 6.0; yeast extract 0.5% (w/v), sucrose 1% (w/v)] according to reference (Malavazi and Goldman, 2012) containing 0.3% of Lallzyme MMX as lytic cocktail and 400 mg of BSA at 30°C (90 rpm). The protoplasts yield was analyzed using Neubauer chamber after 5 h of incubation.

Murine model of pulmonary aspergillosis

The murine model of pulmonary aspergillosis was performed according to (Dinamarco *et al.*, 2012). Outbreed female mice (BALB/c strain; body weight, 20–22 g) were housed in vented cages containing five animals. Mice were immunosuppressed with cyclophosphamide at a concentration of 150 mg per kg of body weight, which was administered intraperitoneally on days −4, −1 and 2 prior to and post infection (day 0). Hydrocortisone acetate (200 mg kg^{-1}) was injected subcutaneously on day −3. The *A. fumigatus* conidia used for inoculation were grown on *Aspergillus* complete YAG for 2 days prior to infection. Fresh conidia were harvested in PBS and filtered through a Miracloth (Calbiochem). Conidial suspensions were spun for 5 min at 3,000 × *g*, washed three times with PBS, counted using a hemocytometer, then resuspended at a concentration of 5.0×10^6 conidia ml^{-1}. Viability counts for the administered inoculum were determined, following serial dilution, and plating on *Aspergillus* YAG, and the conidia were grown at 37°C. Mice were anesthetized by halothane inhalation and infected by intranasal instillation of 1.0×10^5 conidia in 20 μl of PBS. As a negative control, a group of five mice received PBS only. Mice were weighed every 24 h from the day of infection and visually inspected twice daily. In the majority of cases, the endpoint for survival experimentation was identified when a 20% reduction in body weight was recorded, at which time the mice were sacrificed. The statistical significance of comparative survival values was calculated using log rank analysis using the Prism statistical analysis package. Additionally, at 3 days post infection, two mice per strain were sacrificed and the lungs were removed, fixed and processed for histological analysis.

Lung histopathology and fungal burden

After sacrifice, the mice lungs were removed and fixed for 24 h in 3.7% (v/v) formaldehyde-PBS. Samples were washed several times in 70% (v/v) alcohol before dehydration in a series of alcohol solutions of increasing concentrations. Finally, the samples were diafanized in xylol and embedded in paraffin. For each sample, sequential 5-μm-thick sections were collected on glass slides and stained with Gomori methenamine silver (GMS) or hematoxylin and eosin (HE) stain following standard protocols (Greenberger, 2002). Briefly, sections were deparaffinized, oxidized with 4% chromic acid, stained with methenamine silver solution, and counterstained with hematoxylin. Tissue sections were also stained with hematoxylin and eosin for histological examination to determine lung damage. All stained slides were immediately washed, preserved in mounting medium, and sealed with a coverslip. Microscopic analyses were performed using an Axioplan 2 imaging microscope (Carl Zeiss) at the stated magnifications under bright-field conditions.

To investigate fungal burden in the lungs, mice were infected as described previously, but with a higher inoculum of 1×10^6 conidia/20 μl. A higher inoculum, in comparison to the survival experiments, was used to increase fungal DNA detection. Animals were sacrificed 72 h post infection, and both lungs were harvested and immediately frozen in liquid nitrogen. Samples were homogenized by vortexing with glass beads for 10 min, and DNA was extracted via the phenol-chloroform method. DNA quantity and quality were assessed using a NanoDrop 2000 spectrophotometer (Thermo Scientific). At least 500 μg of total DNA from each sample was used for quantitative real-time PCRs. A primer and a Lux probe (Invitrogen) were used to amplify the 18S rRNA region of *A. fumigatus* and an intronic region of mouse GAPDH (glyceraldehyde-3-phosphate dehydrogenase) (Supporting Information Table S3). Six-point standard curves were calculated using serial dilutions of gDNA from all the *A. fumigatus* strains used and the uninfected mouse lung. Fungal and mouse DNA quantities were obtained from the threshold cycle (CT) values from an appropriate standard curve. Fungal burden was determined as the ratio between picograms of fungal and nanograms of mouse DNA.

Determination of TNF-α levels

For cytokine determination, BMDMs from C57BL/6 mice were prepared as previously described (Marim *et al.*, 2010). Briefly, bone marrow cells from femurs of adult mice were cultured for 6 days in RPMI 1640, containing 20% (v/v) fetal bovine serum (FBS) and 30% (v/v) L-929 cell conditioned media (LCCM). Macrophages (5.0×10^5) were plated in 48-well plates for 16 h at 37°C, 5% (v/v) CO_2 in RPMI 140 media containing 10% (v/v) FBS and 5% (v/v) of LCCM. For fungal infection, strains were cultured for 18 h up to a hyphal stage at a density of 2×10^4 per well, UV-irradiated and used to stimulate the macrophages. The cells were centrifuged to synchronize the infection and allowed to infect for 18 h. The supernatant was collected and the cytokine was measured by enzyme-linked immunosorbent assay (ELISA) with a mouse TNF-α kit (R&D Quantikine ELISA) according to the manufacturer's instructions. We have used LPS (1 μg ml^{-1}) for 18 h as a positive control.

Immunoblot analysis

To assess the phosphorylation status of MpkA, fresh harvested conidia (1×10^7) of the wild-type and mutant strains were inoculated in 50 ml liquid YG medium at 37°C for 16 h (180 rpm). Mycelia were ground in liquid nitrogen with pestle and mortar. For protein extraction, 0.5 ml lysis buffer described in (Valiante *et al.*, 2009) containing 10% (v/v) glycerol, 50 mM Tris–HCl pH

7.5, 1% (v/v) Triton X-100, 150 mM NaCl, 0.1% (w/v) SDS, 5 mM EDTA, 50 mM sodium fluoride, 5 mM sodium pyrophosphate, 50 mM β-glycerophosphate, 5 mM sodium orthovanadate, 1 mM PMSF and 1× Complete Mini® protease inhibitor (Roche Applied Science) was added to the ground mycelium. Extracts were centrifuged at 20,000 × *g* for 40 min at 4°C. The supernatants were collected and the protein concentrations were determined using the Bradford method (Bradford, 1976) (BioRad). 50 μg of protein from each sample were resolved in a 12% (w/v) SDS–PAGE and transferred to polyvinylidene difluoride membranes (Merck Millipore). The phosphorylation state and total MpkA was examined using anti-phospho p44/42 MAPK and anti-p44/42 MAPK antibody (9101 and 4370; Cell Signaling Technologies) following the manufacturer's instructions using a 1:1,000 dilution in TBST buffer (137 mM NaCl, 20 mM Tris, 0.1% Tween-20). Primary antibody was detected using an HRP-conjugated secondary antibody raised in rabbit (Sigma). Mouse anti γ-tubulin monoclonal antibody (yN-20; Santa Cruz Biotechnology) was used as loading control in the experiment. It was used in a 1:2,500 dilution in TBST containing 3% (w/v) skimmed milk. Anti γ-tubulin antibody was detected using a monkey peroxidase (HRP)-conjugated second antibody (Santa Cruz Biotechnology). Chemoluminescent detection was achieved using an ECL Prime Western Blot detection kit (GE HealthCare). Images were generated by exposing the membranes to the ChemiDoc™ XRS gel imaging system (BioRad). The images generated were subjected to densitometric analysis using ImageJ software (http://rsbweb.nih.gov/ij/index.html). The MapkA phosphorylation signal was normalized by γ-tubulin and the values of phosphorylation exposure in comparison to the untreated controls were given as percentage. Detection of MpkA phosphorylation in response to CR stress was performed by growing the wild-type and the mutant strains for 16 h at 37°C. Then, CR (300 μg ml^{-1}) was added or not (control) for 15, 30 and 60 min. Detection of MpkA phosphorylation in response to osmotic stress was performed by growing the wild-type and the mutant strains for 16 h at 37°C, prior to addition of 1/2 vol. 3 M sorbitol (Final concentration: 1 M) for 10 min.

Acknowledgements

We would like to thank the Conselho Nacional de Desenvolvimento Científico e Tecnológico (CNPq) and the Fundação de Amparo à Pesquisa do Estado de São Paulo (FAPESP) for providing financial support. We also would like to thank the editor and the four anonymous reviewers and the editor for their comments and suggestions that improve considerably the quality of the manuscript.

References

Aguilera, J., Rodriguez-Vargas, S., and Prieto, J.A. (2005) The HOG MAP kinase pathway is required for the induction of methylglyoxal-responsive genes and determines methylglyoxal resistance in *Saccharomyces cerevisiae*. *Mol Microbiol* **56**: 228–239.

Alonso-Monge, R., Navarro-García, F., Molero, G., Diez-Orejas, R., Gustin, M., Pla J, *et al.* (1999) Role of the mitogen-activated protein kinase Hog1p in morphogenesis and virulence of *Candida albicans*. *J Bacteriol* **181**: 3058–3068.

Altwasser, R., Baldin, C., Weber, J., Guthke, R., Kniemeyer, O., *et al.* (2015) Network Modeling Reveals Cross Talk of MAP Kinases during Adaptation to Caspofungin Stress in *Aspergillus fumigatus*. *PLoS One* **10**: e0136932.

Bahn, Y.S. (2008) Master and commander in fungal pathogens: the two-component system and the HOG signaling pathway. *Eukaryot Cell* **7**: 2017–2036.

Bahn, Y.S., Kojima, K., Cox, G.M., and Heitman, J. (2005) Specialization of the HOG pathway and its impact on differentiation and virulence of *Cryptococcus neoformans*. *Mol Biol Cell* **16**: 2285–300.

Bermejo C, Rodriguez E, Garcia R, Rodriguez-Peña, J.M., Rodriguez de La Concepción, M.L., Rivas C, *et al.* (2008) The sequential activation of the yeast HOG and SLT2 pathways is required for cell survival to cell wall stress. *Mol Biol Cell* **19**: 1113–1124.

Bilsland, E., Molin, C., Swaminathan, S., Ramne, A., and Sunnerhagen, P. (2004) Rck1 and Rck2 MAPKAP kinases and the HOG pathway are required for oxidative stress resistance. *Mol Microbiol* **53**: 1743–1756.

Bom, V.L., de Castro, P.A., Winkelströter, L.K., Marine, M,. Hori, J.I., Ramalho LN, *et al.* (2015) The *Aspergillus fumigatus sitA* phosphatase homologue is important for adhesion, cell wall integrity, biofilm formation, and virulence. *Eukaryot Cell* **14**: 728–744.

Bradford, M.M. (1976) A rapid and sensitive method for the quantitation of microgram quantities of protein utilizing the principle of protein-dye binding. *Anal Biochem* **72**: 248–254.

Brakhage, A.A. (2005) Systemic fungal infections caused by *Aspergillus* species: epidemiology, infection process and virulence determinants. *J Curr Drug Targets* **6**: 875–886.

Brewster, J.L., and Gustin, M.C. (2014) Hog1: 20 years of discovery and impact. *Sci Signal* **7**: re7.

Brown, A.N., and Goldman, G.H. (2016) The contribution of *Aspergillus fumigatus* stress responses to virulence and fungicide resistance. *J Microbiol* **54**: 243–253.

Brown, G.D., Denning, D.W., and Levitz, S.M. (2012a) Tackling human fungal infections. *Science* **336**: 647.

Brown, G.D., Denning, D.W., Gow, N.A., Levitz, S.M., Netea, M.G., and White, T.C. (2012b) Hidden killers: human fungal infections. *Sci Transl Med* **4**: 165rv13.

Carberry, S., Molloy, E., Hammel, S., O'Keeffe, G., Jones, G.W., Kavanagh, K., and Doyle, S. (2012) Gliotoxin effects on fungal growth: mechanisms and exploitation. *Fungal Genet Biol* **49**: 302–312.

Chen, S.C., Slavin, M.A., and Sorrell, T.C. (2011) Echinocandin antifungal drugs in fungal infections: a comparison. *Drugs* **71**: 11–41.

Chen, Y., Zhu, J., Ying, S.H., and Feng, M.G. (2014) Three mitogen-activated protein kinases required for cell wall integrity contribute greatly to biocontrol potential of a fungal entomopathogen. *PLoS One* **9**: e87948.

Chotirmall, S.H., Mirkovic, B., Lavelle, G.M., and McElvaney, N.G. (2014) Immunoevasive *Aspergillus* virulence factors. *Mycopathologia* **178**: 363–370.

de Castro, P.A., Chen, C., de Almeida, R.S., Freitas, F.Z., Bertolini, M.C., Morais, E.R., *et al.* (2014) ChIP-seq

reveals a role for CrzA in the *Aspergillus fumigatus* high-osmolarity glycerol response (HOG) signalling pathway. *Mol Microbiol* **94**: 655–674.
Del Vescovo, V., Casagrande, V., Bianchi, M.M., Piccinni, E., Frontali, L., Militti, C., *et al*. (2008) Role of Hog1 and Yaf9 in the transcriptional response of *Saccharomyces cerevisiae* to cesium chloride. *Physiol Genomics* **33**: 110–120.
Delgado-Jarana, J., Sousa, S., González, F., Rey, M., and Llobell, A. (2006) ThHog1 controls the hyperosmotic stress response in *Trichoderma harzianum*. *Microbiology* **152**: 1687–1700.
Dinamarco, T.M., Almeida, R.S., de Castro, P.A., Brown, N.A., dos Reis, T.F., Ramalho, L.N., *et al*. (2012). Molecular characterization of the putative transcription factor SebA involved in virulence in *Aspergillus fumigatus*. *Eukaryot Cell* **11**: 518–531.
Ding, C., Festa, R.A., Sun, T.S., and Wang, Z.Y. (2014) Iron and copper as virulence modulators in human fungal pathogens. *Mol Microbiol* **93**: 10–23.
Du, C., Sarfati, J., Latgé, J.P., and Calderone, R. (2006) The role of the sakA (Hog1) and tcsB (sln1) genes in the oxidant adaptation of *Aspergillus fumigatus*. *Med Mycol* **44**: 211–218.
Dagenais, T.R., and Keller, N.P. (2009) Pathogenesis of *Aspergillus fumigatus* in Invasive Aspergillosis. *Clin Microbiol Rev* **22**: 447–465.
Ene, I.V., Walker, L.A., Schiavone, M., Lee, K.K., Martin-Yken, H., Dague, E., *et al*. (2015) Cell wall remodeling enzymes modulate fungal cell wall elasticity and osmotic stress resistance. *mBio* **6**: e00986.
Faro-Trindade, I., Willment, J.A., Kerrigan, A.M., Redelinghuys, P., Hadebe, S., Reid, D.M., *et al*. (2012) Characterisation of innate fungal recognition in the lung. *PLoS One* **7**: e35675.
Graham, L.M., Tsoni, S.V., Willment, J.A., Williams, D.L., Taylor, P.R., Gordon, S., *et al*. (2006) Soluble Dectin-1 as a tool to detect beta-glucans. *J Immunol Methods* **314**: 164–169.
Grahl, N., Shepardson, K.M., Chung, D., Jr., and Cramer, R.A. (2012) Hypoxia and fungal pathogenesis: to air or not to air? *Eukaryot Cell* **11**: 560–570.
Greenberger, P.A. (2002) Allergic bronchopulmonary aspergillosis. *J Allergy Clin Immunol* **110**: 685–692.
Haas, H. (2014) Fungal siderophore metabolism with a focus on *Aspergillus fumigatus*. *Nat Prod Rep* **31**: 1266–1276.
Hagiwara, D., Suzuki, S., Kamei, K., Gonoi, T., and Kawamoto, S. (2014) The role of AtfA and HOG MAPK pathway in stress tolerance in conidia of *Aspergillus fumigatus*. *Fungal Genet Biol* **73**: 138–149.
Hagiwara, D., Takahashi-Nakaguchi, A., Toyotome, T., Yoshimi, A., Abe, K., Kamei, K., *et al*. (2013) NikA/TcsC histidine kinase is involved in conidiation, hyphal morphology, and responses to osmotic stress and antifungal chemicals in *Aspergillus fumigatus*. *PLoS One* **8**: e80881.
Hartmann, T., Sasse, C., Schedler, A., Hasenberg, M., Gunzer, M., and Krappmann, S. (2011) Shaping the fungal adaptome-stress responses of Aspergillus fumigatus. *Int J Med Microbiol* **301**: 408–416.
Hayashi, N., Nomura, T., Sakumoto, N., Mukai, Y., Kaneko, Y., Harashima, S., and Murakami, S. (2005) The SIT4 gene, which encodes protein phosphatase 2A, is required for telomere function in *Saccharomyces cerevisiae*. *Curr Genet* **47**: 359–367.
Heinekamp, T., Thywißen, A., Macheleidt, J., Keller, S., Valiante, V., and Brakhage A.A. (2013) *Aspergillus fumigatus* melanins: interference with the host endocytosis pathway and impact on virulence. *Front Microbiol* **3**: 440.
Hohl, T.M., Van Epps, H.L., Rivera, A., Morgan, L.A., Chen, P.L., and Feldmesser, M. (2005) *Aspergillus fumigatus* triggers inflammatory responses by stage specific beta-glucan display. *PLoS Pathog* **1**: e30.
Huang, H., Ostroff, G.R., Lee, C.K., Wang, J.P., Specht, C.A., and Levitz, S.M. (2009) Distinct patterns of dendritic cell cytokine release stimulated by fungal beta-glucans and toll-like receptor agonists. *Infect Immun* **77**: 1774–1781.
Igbaria, A., Lev, S., Rose, M.S., Lee, B.N., Hadar, C.A., Degani, O., and Horwitz, B.A. (2008) Distinct and combined roles of the MAP kinases of *Cochliobolus heterostrophus* in virulence and stress responses. *Mol Plant Microbe Interact* **21**: 769–780.
Kaba, H.E., Nimtz, M., Müller, P.P., and Bilitewski, U. (2013) Involvement of the mitogen activated protein kinase Hog1p in the response of *Candida albicans* to iron availability. *BMC Microbiol* **13**: 16.
Kafer, E. (1977) Meiotic and mitotic recombination in *Aspergilllus* and its chromosomal aberrations. *Adv Genet* **19**: 33–131.
Komalapriya, C., Kaloriti, D., Tillmann, A.T, Yin, Z., Herrero-de-Dios, C., Jacobsen, M.D., *et al*. (2015) Integrative model of oxidative stress adaptation in the fungal pathogen *Candida albicans*. *PLoS One* **10**: e0137750.
Lackner, M., and Lass-Flörl, C. (2013) Up-date on diagnostic strategies of invasive aspergillosis. *Curr Pharm Des* **19**: 3595–3614.
Lawrence, C.L., Botting, C.H., Antrobus, R., and Coote, P.J. (2004) Evidence of a new role for the high-osmolarity glycerol mitogen-activated protein kinase pathway in yeast: regulating adaptation to citric acid stress. *Mol Cell Biol* **24**: 3307–3323.
Liang, S.H., Cheng, J.H., Deng, F.S., Tsai, P.A., and Lin, C.H. (2014) A novel function for Hog1 stress-activated protein kinase in controlling white-opaque switching and mating in *Candida albicans*. *Eukaryot Cell* **13**: 1557–1566.
Lin, C.H., and Chung, K.R. (2010) Specialized and shared functions of the histidine kinase- and HOG1 MAP kinase-mediated signaling pathways in *Alternaria alternata*, a filamentous fungal pathogen of citrus. *Fungal Genet Biol* **47**: 818–827.
Ma D, and Li R. (2013) Current understanding of HOG-MAPK pathway in *Aspergillus fumigatus*. *Mycopathologia* **175**: 13–23.
Maeda, T., Wurgler-Murphy, S.M., and Saito, H. (1994) A two-component system that regulates an osmosensing MAP kinase cascade in yeast. *Nature* **369**: 242–245.
Malavazi, I., and Goldman, G.H. (2012) Gene disruption in *Aspergillus fumigatus* using a PCR-based strategy and in vivo recombination in yeast. *Methods Mol Biol* **845**: 99–118.
Marim, F.M., Silveira, T.N., Lima, D.S., Jr., and Zamboni, D.S. (2010) A method for generation of bone marrow-

derived macrophages from cryopreserved mouse bone marrow cells. *PloS One* **5**: e15263.
McCormick, A., Jacobsen, I.D., Broniszewska, M., Beck, J., Heesemann, J., Ebel, F. (2012) The two-component sensor kinase TcsC and its role in stress resistance of the human-pathogenic mold *Aspergillus fumigatus*. *PLoS One* **7**: e38262.
Mollapour, M, and Piper, PW (2006) Hog1p mitogen-activated protein kinase determines acetic acid resistance in *Saccharomyces cerevisiae*. *FEMS Yeast Res* **6**: 1274–1280.
Monge, R.A., Román, E., Nombela, C., and Pla, J. (2006) The MAP kinase signal transduction network in *Candida albicans*. *Microbiology* **152**: 905–912.
Moore, M.M. (2013) The crucial role of iron uptake in *Aspergillus fumigatus* virulence. *Curr Opin Microbiol* **16**: 692–699.
Mowat, E., Butcher, J., Lang, S, Williams, C., and Ramage, G. (2007) Development of a simple model for studying the effects of antifungal agents on multicellular communities of *Aspergillus fumigatus*. *J Med Microbiol* **56**: 1205–1212.
Nimmanee, P., Woo, P.C., Kummasook, A., and Vanittanakom, N. (2015) Characterization of *sakA* gene from pathogenic dimorphic fungus *Penicillium marneffei*. *Int J Med Microbiol* **305**: 65–74.
Panadero, J., Pallotti, C., Rodríguez-Vargas, S., Randez-Gil, F., and Prieto, J.A. (2006) A downshift in temperature activates the high osmolarity glycerol (HOG) pathway, which determines freeze tolerance in Saccharomyces cerevisiae. *J Biol Chem* **281**:4638–4645.
Park, S.M., Choi, E.S., Kim, M.J., Cha, B.J., Yang, M.S., and Kim, D.H. (2004) Characterization of HOG1 homologue, CpMK1, from *Cryphonectria parasitica* and evidence for hypovirus-mediated perturbation of its phosphorylation in response to hypertonic stress. *Mol Microbiol* **51**: 1267–1277.
Pearson, G., Robinson, F., Beers Gibson, T., Xu, B.E., Karandikar, M., Berman, K., and Cobb, M.H. (2001) Mitogen-activated protein (MAP) kinase pathways: regulation and physiological functions. *Endocr Rev* **22**: 153–183.
Rodríguez-Peña, J.M., García, R., Nombela, C., and Arroyo, J. (2010) The high-osmolarity glycerol (HOG) and cell wall integrity (CWI) signalling pathways interplay: a yeast dialogue between MAPK routes. *Yeast* **27**: 495–502.
Reyes, G., Romans, A., Nguyen, C.K., and May, G.S. (2006) Novel mitogen-activated protein kinase MpkC of *Aspergillus fumigatus* is required for utilization of polyalcohol sugars. *Eukaryot Cell* **5**: 1934–1940.
Rispail, N., Soanes, D.M., Ant, C., Czajkowski, R., Grünler, A., Huguet, R., *et al*. (2009) Comparative genomics of MAP kinase and calcium-calcineurin signalling components in plant and human pathogenic fungi. *Fungal Genet Biol* **46**: 287–298.
Rocha, M.C., Godoy, K.F., de Castro, P.A., Hori, J.I., Bom, V.L., Brown, N.A., *et al*. (2015) The *Aspergillus fumigatus* pkcAG579R mutant is defective in the activation of the cell wall integrity pathway but is dispensable for virulence in a neutropenic mouse infection model. *PLoS One* **10**: e0135195.
Román, E., Arana, D.M., Nombela, C., Alonso-Monge, R., and Pla, J. (2007) MAP kinase pathways as regulators of fungal virulence. *Trends Microbiol* **15**: 181–190.
Saito H, and Posas F. (2012) Response to hyperosmotic stress. *Genetics* **192**: 289–318.
Scharf, D.H., Heinekamp, T., Remme, N., Hortschansky, P., Brakhage, A.A., and Hertweck, C. (2012) Biosynthesis and function of gliotoxin in *Aspergillus fumigatus*. *Appl Microbiol Biotechnol* **93**: 467–472.
Schrettl M., and Haas, H. (2011) Iron homeostasis-Achilles' heel of *Aspergillus fumigatus*? *Curr Opin Microbiol* **14**: 400–405.
Segmuller, N., Ellendorf, U., Tudzynski, B., and Tudzynski, P. (2007) BcSAK1, a stress-activated mitogen-activated protein kinase, is involved in vegetative differentiation and pathogenicity in *Botrytis cinerea*. *Eukaryot Cell* **6**: 211–221.
Shopova, I., Bruns, S., Thywissen, A., Kniemeyerm, O. Brakhage, A.A., and Hillmann, F. (2013) Extrinsic extracellular DNA leads to biofilm formation and colocalizes with matrix polysaccharides in the human pathogenic fungus *Aspergillus fumigatus*. *Front Microbiol* **4**: 141.
Steele, C., Rapaka, R.R., Metz, A., Pop, S.M., Williams, D.L., Gordon, S., *et al*. (2005) The beta-glucan receptor dectin-1 recognizes specific morphologies of *Aspergillus fumigatus*. *PLoS Pathog* **1**: e42.
Sugui, J.A., Kwon-Chung, K.J., Juvvadi, P.R., Latgé, J.P., and Steinbach, W.J. (2014) *Aspergillus fumigatus* and related species. *Cold Spring Harb Perspect Med* **5**: a019786.
Taramelli, D., Malabarba, M.G., Sala, G., Basilico, and Cocuzza, G. (1996) Production of cytokines by alveolar and peritoneal macrophages stimulated by *Aspergillus fumigatus* conidia or hyphae. *J Med Vet Mycol* **34**: 49–56.
Tekaia, F., and Latgé, J.P. (2005) *Aspergillus fumigatus*: saprophyte or pathogen? *Curr Opin Microbiol* **8**: 385–392.
Thomas, E., Roman, E., Claypool, S., Manzoor, N., Pla, J., and Panwar, S.L. (2013) Mitochondria influence CDR1 efflux pump activity, Hog1-mediated oxidative stress pathway, iron homeostasis, and ergosterol levels in *Candida albicans*. *Antimicrob Agents Chemother* **57**: 5580–5599.
Thorsen, M., Di, Y., Tängemo, C., Morillas, M., Ahmadpour, D., Van der Does, C., *et al*. (2006) The MAPK Hog1p modulates Fps1p-dependent arsenite uptake and tolerance in yeast. *Mol Biol Cell* **17**: 4400–4410.
Van Thuat, N., Schafer, W., and Bormann, J. (2012) The stress-activated protein kinase FgOS-2 is a key regulator in the life cycle of the cereal pathogen *Fusarium graminearum*. *Mol Plant Microbe Interact.* **25**: 1142–1156.
Valiante, V., Macheleidt, J., Föge, M., and Brakhage, A.A. (2015a) The *Aspergillus fumigatus* cell wall integrity signaling pathway: drug target, compensatory pathways, and virulence. *Front Microbiol* **6**: 325.
Valiante, V., Monteiro, M.C., Martín, J., Altwasser, R., El Aouad, N., González, I., *et al*. (2015b) Hitting the Caspofungin Salvage pathway of human-pathogenic fungi with the novel lasso peptide humidimycin (MDN-0010). *Antimicrob Agents Chemother* **59**: 5145–5153.
Valiante, V., Heinekamp, T., Jain, R., Härtl, A., and Brakhage, A.A. (2008) The mitogen-activated protein kinase MpkA of Aspergillus fumigatus regulates cell wall signaling and oxidative stress response. *Fungal Genet Biol* **45**:618–627.
Valiante, V., Jain, R., Heinekamp, T., and Brakhage, A.A (2009) The MpkA MAP kinase module regulates cell wall

integrity signaling and pyomelanin formation in *Aspergillus fumigatus*. *Fungal Genet Biol* **46**: 909–918.
Wezensky, S.J., Jr., and Cramer, R.A. (2011) Implications of hypoxic microenvironments during invasive aspergillosis. *Med Mycol* **49**(Suppl 1): S120–S124.
Winkelströter, L.K., Bom, V.L., de Castro, P.A., Ramalho, L.N., Goldman, M.H., Brown, N.A., *et al*. (2015a) High osmolarity glycerol response PtcB phosphatase is important for *Aspergillus fumigatus* virulence. *Mol Microbiol* **96**: 42–54.
Winkelströter, L.K., Dolan, S.K., Dos Reis T.F., Bom, V.L., Alves de Castro, P., Hagiwara, D., *et al*. (2015b) Systematic global analysis of genes encoding protein phosphatases in *Aspergillus fumigatus*. *G3 (Bethesda)* **5**: 1525–1539.
Winkler, A., Arkind, C., Mattison, C.P., Burkholder, A., Knoche, K., and Ota, I. (2002) Heat stress activates the yeast high-osmolarity glycerol mitogen-activated protein kinase pathway, and protein tyrosine phosphatases are essential under heat stress. *Eukaryot Cell* **1**: 163–173.
Zhang, Y., Zhao, J., Fang, W., Zhang, J., Luo, Z., Zhang, M., *et al*. (2009) Mitogen-activated protein kinase hog1 in the entomopathogenic fungus Beauveria bassiana regulates environmental stress responses and virulence to insects. *Appl Environ Microbiol* **75**: 3787–3795.

Supporting information

Additional supporting information may be found in the online version of this article at the publisher's web-site.